1970

The design and construction of a constant acceleration drive system for Mössbauer experiments

James Donald Russell
University of the Pacific

THE DESIGN AND CONSTRUCTION OF A CONSTANT ACCELERATION DRIVE SYSTEM FOR MÖSSBAUER EXPERIMENTS

A Thesis

Presented to

the Faculty of the Department of Physics

College of the Pacific

University of the Pacific

In Partial Fulfillment

of the Requirements for the Degree

Master of Science in Physics

---

by

James Donald Russell

March 1970

This thesis, written and submitted by

James Donald Russell ,

is approved for recommendation to the

Graduate Council, University of the Pacific.

Department Chairman or Dean:

Carl E Wellman

Thesis Committee:

Andrés Rodríguez F., Chairman

Fred W. Inman

Calvin Potts

Carl E Wellman

Dated March 31, 1970

TABLE OF CONTENTS

LIST OF TABLES

LIST OF FIGURES

LIST OF FIGURES, CONTINUED

CHAPTER I

THE MÖSSBAUER EFFECT

An excited nucleus may undergo a transition to its ground state by the emission of a gamma ray. The nucleus, if free to do so, will recoil and take some of the transition energy as recoil energy leaving less energy for the emitted gamma ray. This gamma ray does not have enough energy to excite a similar nucleus and will, therefore, not be resonantly absorbed due to the fact that the natural linewidth of the gamma ray is so much smaller than the energy taken by the emitting atom and the similar energy needed by the absorbing atom.

In 1958 a new effect in the emission and absorption processes of low energy gamma rays was announced by Rudolph L. Mössbauer.[1] His discovery was made while he was doing graduate work at Heidelberg, Germany. Since that time this effect, now known as the Mössbauer effect, has been studied and confirmed in many laboratories. By 1961 the significance

---

[1] Rudolph L. Mössbauer, "Kernresonanzfluoreszenz von Gammastrahlund in Ir^{191}," Die Naturwissenschafter, Vol. 45 (1958), pp. 538-539; Rudolph L. Mössbauer, "Kernresonanzfluoreszenz von Gammastrahlund in Ir^{191}," Zeitschrift fur Physik, Vol. 151 (1958), pp. 124-143; Rudolph L. Mössbauer, "Kernresonanzabsorption von Gammastrahlund in Ir^{191}," Z. Naturforsch, Vol. 14a (1959), p. 211.

and usefulness of this effect was so widely recognized that Rudolph Mössbauer was awarded the Nobel Prize.[2]

The new effect involves recoil free emission and resonant absorption of low energy gamma rays by atoms tightly bound in a crystalline lattice. The characteristics of the Mössbauer effect have lead to the feasibility of studies previously not possible in nuclear-, solid state-, and atomic physics; chemistry; and biology.

It is the purpose of this research project to design and build a Mössbauer effect apparatus.

Theory and Application

Nuclear absorption of gamma rays is not easily observed because of the interaction of the photons with the atomic electrons in photoelectric and Compton effects. The absorption of a gamma ray into the nucleus can be observed if it results in some nuclear reaction. Of interest is the attempt to observe nuclear resonance absorption. This phenomenon is difficult to observe because the energies of the emitted and absorbed gamma rays do not coincide and are different from the transition energy by an amount equal to the recoil energy taken by the nucleus, $E_r = E^2/2Mc^2$.

---

[2]Rudolph L. Mössbauer, "Les Prix Nobel En 1961, Nobel Foundation Stockholm, 1962," Science, Vol, 137 (1962), pp. 731-738.

(For the 14.4 kev transition in Fe^{57} this recoil energy amounts to 2×10^{-3}ev.) The emitted gamma ray energy is less than the transition energy by the amount E_r, and the absorbed gamma ray must have an energy greater than the transition energy by an amount E_r.

Nuclei have very highly defined energy levels and the radiations given off in transitions from an excited state to a ground state will all have about the same energy. The natural linewidth, Γ, of the resulting radiation is obtained from the uncertainty principle

$$\Gamma\tau = \hbar$$

or

$$\Gamma = \frac{0.693}{t_{1/2}}\hbar$$

From which we see that a half-life of 1.0×10^{-7}sec (corresponding to the Fe^{57} metastable state) leads to a linewidth of 4.6×10^{-9}ev. By considering the ratio of this linewidth to the total energy of the gamma ray,

$$\frac{\Gamma}{E} = \frac{4.6 \times 10^{-9}\ e.v.}{14.4 \times 10^{3}\ e.v} = 3 \times 10^{-13}$$

we see that the energy of the gamma ray is defined to within three parts in 10^{13}, one of the most accurately defined energies.

The natural linewidth is six orders of magnitude smaller than the energy E_r taken by the recoiling nucleus, and therefore the emission and absorption lines do not overlap. Thus, resonant absorption is not observed unless the recoil

energy loss is made up. This was demonstrated by P.B. Moon[3] who shifted the gamma ray energy by applying the Doppler effect to bring about resonant scattering.

Atoms which are bound in a crystalline lattice, will be dislodged from their lattice sites if their free-atom recoil energy is larger than their lattice binding energy, 15-30ev.[4] However, if the recoil energy is not larger than the binding energy, the recoil energy will be dissipated by the transfer of integral multiples of phonon energy $(0, \pm\hbar w, \pm 2\hbar w, \ldots)$ to the lattice,[5] and the effective line-width is of the order of the phonon energies.

If the recoil energy is less than the phonon energy (on the order of 10^{-2}ev), there will be the possibility of zero phonon energy transfer, and the gamma ray will come off with effectively the full energy of the transition. In this case the recoil momentum accompanying emission or absorption of a gamma ray is taken up by a large number of the atoms in the crystal, rather than by a single nucleus. Even for a minute crystal of Fe^{57} (e.g., $1\mu^3$ crystal contains

---

[3]P. B. Moon, Proc. Phys. Soc. A64 (1951), p. 76.

[4]Gunther K. Wertheim, Mössbauer Effect: Principles and Applications (New York: Academic Press, 1964), p. 8.

[5]Ibid., p. 9.

about 10^{11} atoms), the recoil energy is

$$E_r = \frac{E^2}{2Mc^2} = 2 \times 10^{-14} ev$$

for the 14.4 kev transition. This is extremely small, much smaller than the natural linewidth of the gamma rays, and thus resonant absorption can be observed. It is these zero phonon events which constitute the Mössbauer effect.

If the zero phonon gamma ray energy is shifted such that it falls outside the natural linewidth of the absorbing nucleus, reabsorption again becomes impossible. This shift in gamma ray energy can be obtained by subjecting the gamma ray to a Doppler effect. This can be accomplished by relative motion between the emitting crystal and the absorbing crystal. If the emitting crystal is moving toward the absorbing crystal with a velocity ,v, the gamma ray energy is changed by an amount

$$\delta E = \frac{E v}{c} .$$

It only takes a velocity $v = 10^{-2}$cm/sec to shift the gamma ray energy by one linewidth, and it will take twice this velocity to overcome the linewidth of both the source and the absorber and thus cancel out resonance.

It has been found that the excited state of Fe^{57} has a most advantageous combination of half-life, recoil energy, and phonon energy to permit the Mössbauer effect. Fe^{57} also

has a cross section for resonant absorption of gamma rays of $2.2 \times 10^{-18} cm^2$. This is about two hundred times larger than for photoelectric absorption, the second most important process.[6] Fe^{57} comes from the decay of Co^{57}, as is illustrated in Figure 1. The 14.4 kev transition is the one probably most often used in Mössbauer experiments and is the one which will be used here. The source for this research is Co^{57} imbedded in Platinum.

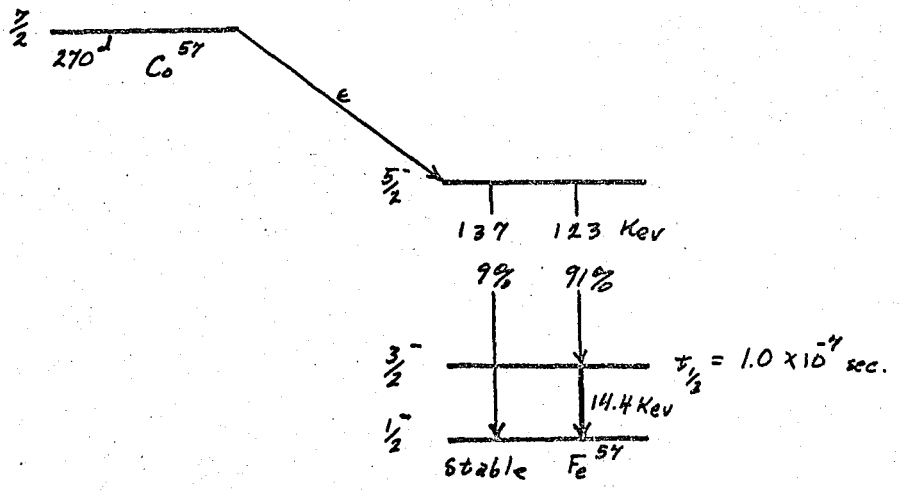

Figure 1. The Decay of Co^{57} to Fe^{57}.

The Mössbauer effect can be used in the study of processes which cause shifts in gamma ray energy or in nuclear energy levels.

According to the theory of special relativity, a photon

---

[6] Gunther K. Wertheim. Mössbauer Effect: Principles and Applications (New York: Academic Press, 1964), p. 8.

should undergo a shift in energy due to its interaction with a gravitational field.[7] Investigation of the gravitational red shift showed the predicted effect of gravity upon a photon and thus added additional experimental evidence for the theory of special relativity.[8]

Processes which cause shifts in nuclear energy levels can be investigated by the study of (1) isomer shift, (2) quadrupole coupling, and (3) magnetic hyperfine structure. All of these are due to the interaction of the nucleus with the surrounding electrons.

The isomer shift, also known as the "chemical shift", is caused in part by a difference in the s-electron density at the nuclear site of each participating atom and in part by a difference in the effective radii of the energy states. The nuclear energy levels are shifted by the electrostatic interaction of the nucleus with the orbital electrons. The electrostatic potential for a point nucleus is

$$V_{pt} = \frac{Ze}{r}$$

whereas for a finite spherical nucleus of radius ,R, and of uniform charge density, the potential becomes

---

[7] Robert Resnick, Introduction to Special Relativity (New York: John Wiley & Sons, Inc., 1968), p. 212

[8] R. V. Pound, G.A. Rebka, Jr., "Apparent Weight of Photons," Phys. Rev. Letters, Vol. 4, No. 337 (1960); R.V. Pound, J.L. Snider, "Effects of Gravity on Gamma Radiation," Phys. Rev. Letters, Vol. 140, B-788 (1965).

$$V = \frac{Ze}{R}\left[\frac{3}{2} - \frac{r^2}{2R^2}\right], \quad \text{for} \quad r \leq R$$

and

$$V = \frac{Ze}{r}, \quad \text{for} \quad r \geq R.$$

When emersed in a uniform electron cloud of density, ρ, there is an energy difference between a finite nucleus and a point nucleus given by the integral,[9]

$$\begin{aligned}\delta E &= \int_0^{2\pi}\int_0^{\pi}\int_0^{\infty}(V - V_{pt})\rho\, r^2 \sin\theta\, dr\, d\theta\, d\phi \\ &= 4\pi\rho\int_0^{\infty}(V - V_{pt})\, r^2 dr \\ &= \frac{4\pi\rho Ze}{R}\int_0^{R}\left(\frac{3}{2} - \frac{r^2}{2R^2} - \frac{R}{r}\right) r^2 dr \\ &= -\frac{2}{5}\pi Ze\rho R^2 = \frac{2}{5}\pi Z e^2 |\psi_{(0)}|^2 R^2\end{aligned}$$

where in the last step we replace ρ with

$$\rho = -e|\psi_{(0)}|^2$$

This expression predicts a raising of all nuclear energy levels according to the radius of the energy state and permits an effect upon the energy levels according to the electron density, which is subject to chemical changes. In other words, the ground state and all excited states of a nucleus are shifted by such an amount, called the isomeric shift. The nucleus in an excited state has a larger charge radius and therefore a larger energy level shift. When emitting a gamma ray in a transition from the excited state to the ground state, the gamma ray comes off with the energy difference E_s between

---

[9] Gunther K. Wertheim, Mössbauer Effect: Principles and Applications (New York: Academic Press, 1964), p. 50.

these two isomeric shifted energy levels.

$$E_s = E_o + \delta E_{ex} - \delta E_{gd}$$
$$= E_o + \frac{2}{5}\pi Z e^2 |\psi_{s(0)}|^2 R_{ex}^2 - \frac{2}{5}\pi Z e^2 |\psi_{s(0)}|^2 R_{gd}^2$$
$$= E_o + \frac{2}{5}\pi Z e^2 |\psi_{s(0)}|^2 (R_{ex}^2 - R_{gd}^2).$$

A similar change in the energy levels will have taken place in the absorber where the electron charge density is apt to be different (See Figure 2). The energy of the absorbed gamma ray will be given by a similar expression where the only difference lies in the electron charge density

$$E_a = E_o + \frac{2}{5}\pi Z e^2 |\psi_{a(0)}|^2 (R_{ex}^2 - R_{gd}^2).$$

The isomer shift is the difference in the energies of the emitted and absorbed gamma rays, i.e.,

$$I.S. = E_a - E_s$$
$$= \frac{2}{5}\pi Z e^2 [|\psi_{a(0)}|^2 - |\psi_{s(0)}|^2] (R_{ex}^2 - R_{gd}^2).$$

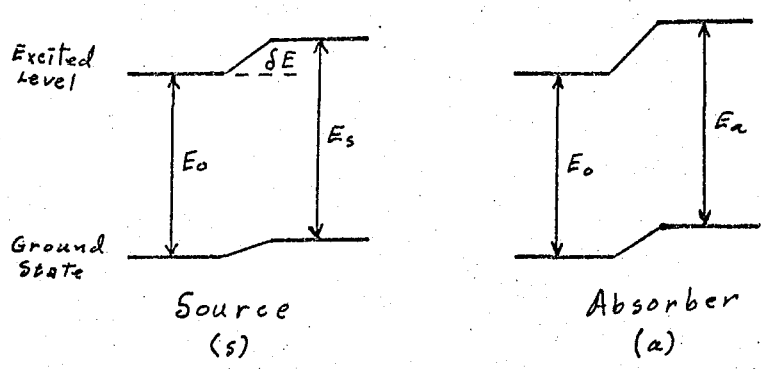

Figure 2. Isomer shift of energy levels in Fe^{57} source and absorber.

If the electron charge densities are the same, there will be no isomer shift; and the emitted gamma ray will be resonantly absorbed. As is generally the case, the electron charge densities will not be the same and to bring the system back to resonance the source is given a velocity which, by the Doppler effect, changes the energy of the emitted gamma ray.

Electric quadrupole coupling[10] is due to the interaction of the nuclear electric quadrupole moment with the electric field gradient at the nuclear site within the crystal. The quadrupole moment of the nucleus appears if the nuclear charge distribution is not spherical, and is dependant upon the nuclear spin quantum number, I.[11] (Nuclei with spin of 0 or 1/2 do not exhibit a quadrupole moment due to their spherical symmetry.) The interaction of the nuclear quadrupole moment, Q, with the electric field gradient leads to a splitting of the nuclear energy levels. This interaction is expressed by the Hamiltonian

$$\mathcal{H} = Q \cdot \nabla E$$

whose eigenvalues

$$E_Q = \frac{e^2 q Q}{4I(2I-1)}\left[3m_I^2 - I(I+1)\right]\left(1 + \eta^2/3\right)^{1/2}$$

---

[10] T.P. Das, E.L. Hahn, Nuclear Quadrupole Resonance Spectroscopy (New York: Academic Press Inc.,(1958).

[11] Robert A. Howard, Nuclear Physics (Belmont: Wadsworth Publishing Company, Inc., 1963), pp. 59, 135.

give the amount of splitting. The η is an asymmetry parameter which permits application to non-axially symmetric field gradients. And eq is the field gradient in the axial direction (taken as z axis). The m_I is the magnetic quantum number, which can take on the values $m_I = I, I-1, \ldots, -I$.

The equation for E_Q is degenerate for states whose m_I differ in sign only. Thus, the $I = 3/2$ level is split into two levels one for $m_I = \pm 3/2$ and the other for $m_I = \pm 1/2$. These two levels (See Figure3) differ by an amount

$$\Delta E_Q = E_{Q(3/2)} - E_{Q(1/2)}$$
$$= \frac{e^2 q Q}{2}$$

for an axially symetric field gradient.

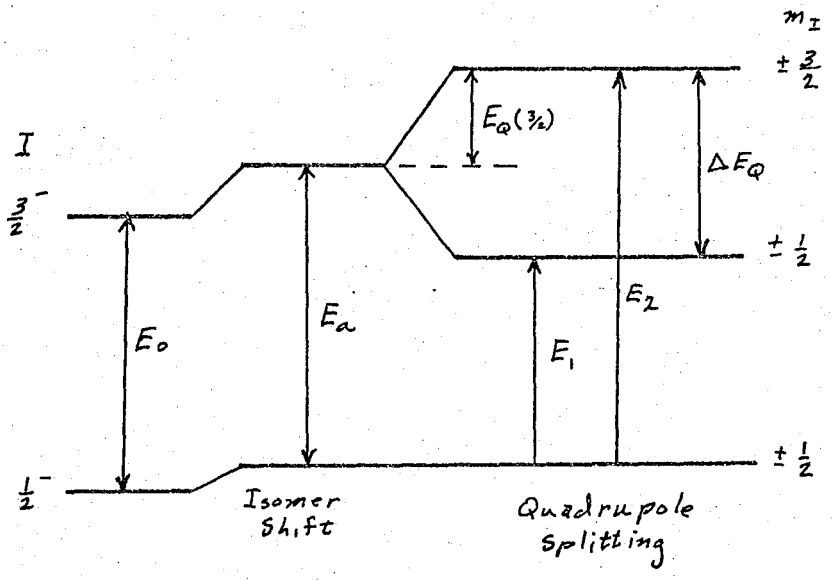

Figure 3. Quadrupole splitting of Fe^{57} energy levels.

In the ground state of Fe^{57}, I = 1/2; and there will be no quadrupole splitting of this level. An absorbed gamma ray will thus need either of the two transition energies,

$$E_1 = E_a + E_Q(\tfrac{1}{2}) = E_a - e^2qQ/4$$

or

$$E_2 = E_a + E_Q(\tfrac{3}{2}) = E_a + e^2qQ/4$$

since the quadrupole interaction splits the isomeric shifted level, as is illustrated in Figure 3. This means that the emitted gamma ray from a single line source (a source with unsplit levels), can be brought into resonance at two different Doppler velocities.

The magnetic hyperfine structure[12] in a nucleus is produced by the relative orientation of the nuclear magnetic dipole moment, μ, in the magnetic field produced by electronic spin and orbital motions. This interaction could properly be called magnetic dipole coupling.

The Hamiltonian stating this interaction is

$$\mathcal{H}_m = -\mu \cdot H$$
$$= -g\mu_n I \cdot H$$

leading to a splitting of the energy levels by the amount

$$E_m = -\mu H m_I/I$$
$$= -g\mu_n H m_I$$

where g is the gyromagnetic ratio, and μ_n is the nuclear magneton. We see that the amount of splitting is directly

---

[12]Gunther K. Wertheim, Mössbauer Effect: Principles and Applications (New York: Academic Press, 1964), p. 72.

proportional to m_I, which means that the ground state energy level will be split into two levels, and the excited state energy level will be split into four levels as is shown in Figure 4.

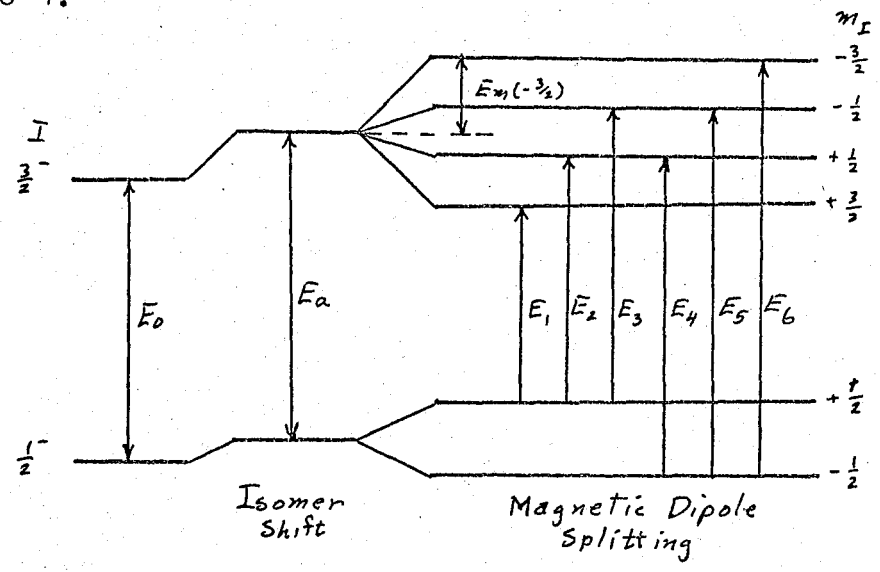

Figure 4. Magnetic hf splitting of the ground and first excited states of Fe^{57}.

A gamma ray resulting from a transition between nuclear energy levels will carry away an amount of angular momentum $L\hbar$, such that the sum of the z component of the angular momentum of the resultant nuclear level and the angular momentum of the gamma ray will be the same as the original nuclear level (conservation of angular momentum). Possible transitions are determined by the equation,

$$|I_1 - I_2| \leq L \leq |I_1 + I_2| \quad , \quad L \neq 0$$

which determines the mode of transition consistent with parity. For transitions between the split nuclear levels $|\Delta m| \leq L$ must be satisfied.

For Fe^{57}, in which I_1 equals $3/2^-$ and I_2 equals $1/2^-$, L is equal to 1 and the gamma ray is of the magnetic dipole form; the type for which L = 1 does not change parity. Since L = 1, $\Delta m = 0, \pm 1$, and the six possible transitions consistent with these criteria are illustrated in Figure 4.

The gamma ray resulting from one of these transitions or, as in our case, inciting one of these transitions upon absorption will have one of the following energies.

$$E_1 = E_a + E_m(+\tfrac{3}{2}) + E_m(+\tfrac{1}{2})$$
$$E_2 = E_a + E_m(+\tfrac{1}{2}) + E_m(+\tfrac{1}{2})$$
$$E_3 = E_a + E_m(-\tfrac{1}{2}) + E_m(+\tfrac{1}{2})$$
$$E_4 = E_a + E_m(+\tfrac{1}{2}) + E_m(-\tfrac{1}{2})$$
$$E_5 = E_a + E_m(-\tfrac{1}{2}) + E_m(-\tfrac{1}{2})$$
$$E_6 = E_a + E_m(-\tfrac{3}{2}) + E_m(-\tfrac{1}{2})$$

The monochromatic gamma ray from a source without nuclear level splitting can be brought into resonant absorption at each of these six energies by applying appropriate Doppler shifts. The resulting hyperfine Mössbauer spectrum is thus a six line spectrum.

Instrumentation

In order to detect when resonant absorption takes place, we must modulate the gamma ray energy over a range including the absorption energies. This is most easily done by applying a varying Doppler shift to the emitted monochromatic

gamma rays; and observing the number of gamma rays transmitted through the absorber as a function of their modulated energy. This yields a Mössbauer absorption spectrum.

CHAPTER II

DESIGN AND CONSTRUCTION OF DRIVE UNIT

There are two approaches to the Doppler Modulation technique: (1) Constant Velocity, and (2) Variable Velocity.

In using the constant velocity technique[13], one stores counts for a predetermined length of time and then increases the velocity by some increment, and the procedure is repeated.

In the variable velocity technique[14], the system sweeps repeatedly through the range of velocities of interest. This type of system requires the use of a multichannel analyzer to sort the counts according to instantaneous velocity. To obtain

---

[13] P.A. Flinn, "Velocity Servo Drive for a High Precision Mössbauer Spectrometer," Rev. Sci. Inst. Vol. 34, No. 12 (1963), pp. 1422-1426; Ruegg, P.C., J.J. Spikkerman, J.R. Devon, "Drift Free Mössbauer Spectrometer," Rev. Sci. Inst., Vol. 36, No. 3 (March 1965), pp. 356-359; J. Blipkin, and others, "Inexpensive Automatic Recording Mössbauer Spectrometer," Rev. Sci. Inst. Vol. 35, No. 10 (October 1964), pp. 1336-1339.

[14] E. Kankeleit, "Velocity Spectrometer for Mössbauer Experiments," Rev. Sci. Inst., Vol. 35, No. 2 (February 1964), pp. 194-197; David Rubin, "Constant Acceleration Transducer Employing Negative Feedback for Use in 'Mössbauer Experiments'," Rev. Sci. Inst, Vol. 33, No. 12 (December, 1962), pp. 1358-1360; F.C. Ruegg, J.J. Spikkerman, J.R. DeVoe, "Drift Free Mössbauer Spectrometer," Rev. Sci. Inst, Vol. 36, No. 3 (March 1965), pp. 356-359; R.L. Cohen, P.G. McMullin, G.K. Wertheim, "High Velocity Drive for Mössbauer Experiments," Rev. Sci. Inst. Vol. 34, No. 6 (June 1963), pp. 671-673; R.L. Cohen, "Improvements on Electromagnetic Velocity Drive for Mössbauer Experiments," Rev. Sci. Inst., Vol. 37, No. 7 (July 1966), pp. 957-959.

this data in the most convenient form requires that we maintain a linear velocity scale and a flat nonabsorption spectrum, which means that equal lengths of time must be spent in equal velocity increments. That is, we maintain constant acceleration. Having available a multichannel analyzer readily adaptable to the requirements of constant accelerated motion, this type of drive system will be used.

The Drive Unit

The drive unit (Figures 5,6) consists of a loud speaker driver [15] mechanically coupled to a velocity transducer. Mechanical coupling is achieved through the use of a 3/16 inch brass rod, one end of which is attached to the voice coil of the speaker. The other end is attached to a short length of magnetized iron rod centrally located in the velocity transducer. Another piece of 3/16 inch brass rod is then attached to the other end of this magnetic rod and extends out the further end of the velocity transducer. The radioactive source (Co^{57}) is mounted on the distal end of this piece of rod. This three-piece rod is supported near each end by a three wire system. Many commercial or locally constructed drive systems employ the use of elaborate punched phosphore-bronze support spiders, but not having the facilities to make such items, it was necessary to develop

---

[15] Oaktron 12H3 (Chosen for its low cost, about $7.00).

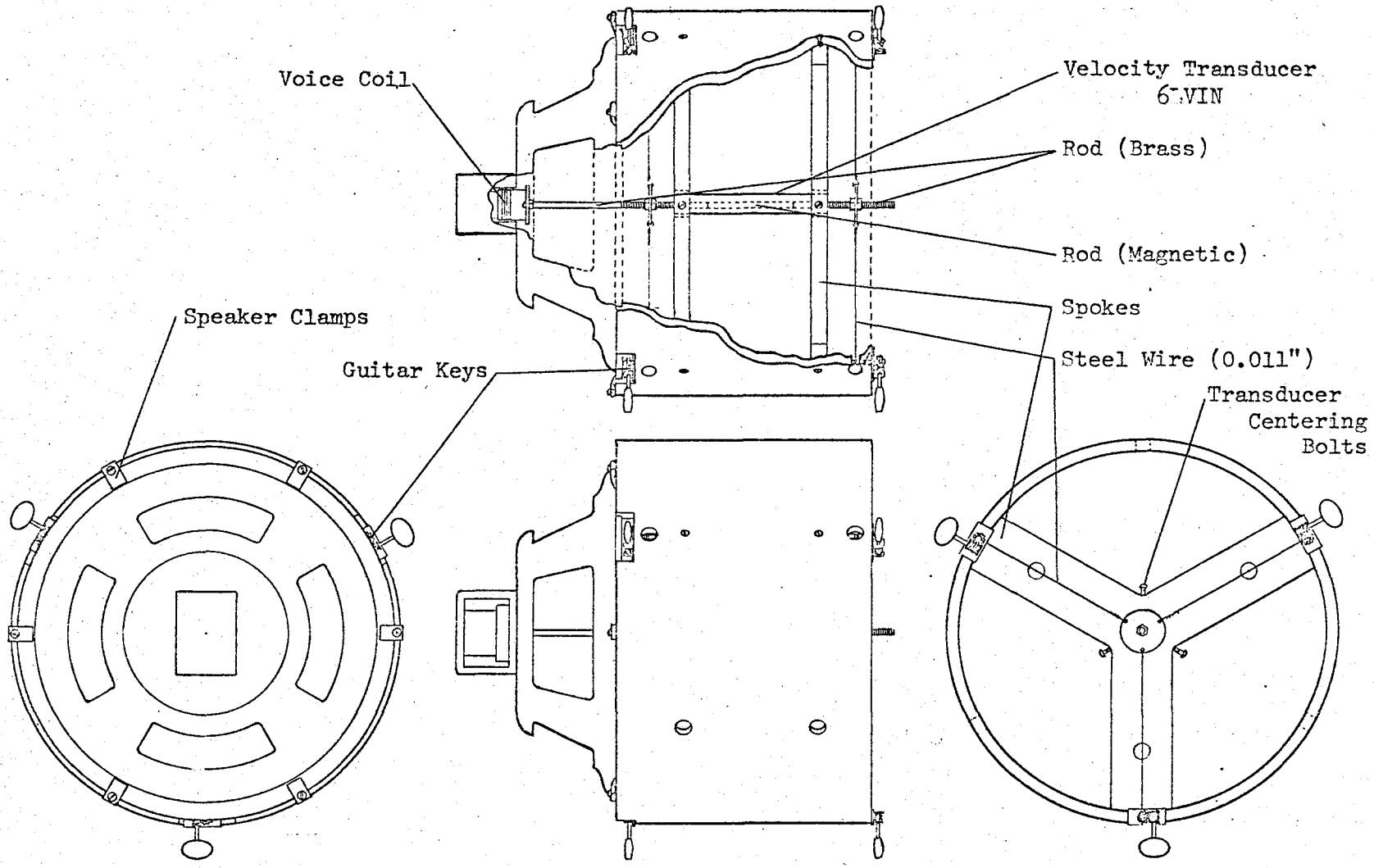

Figure 5. Diagram of Drive Unit Construction

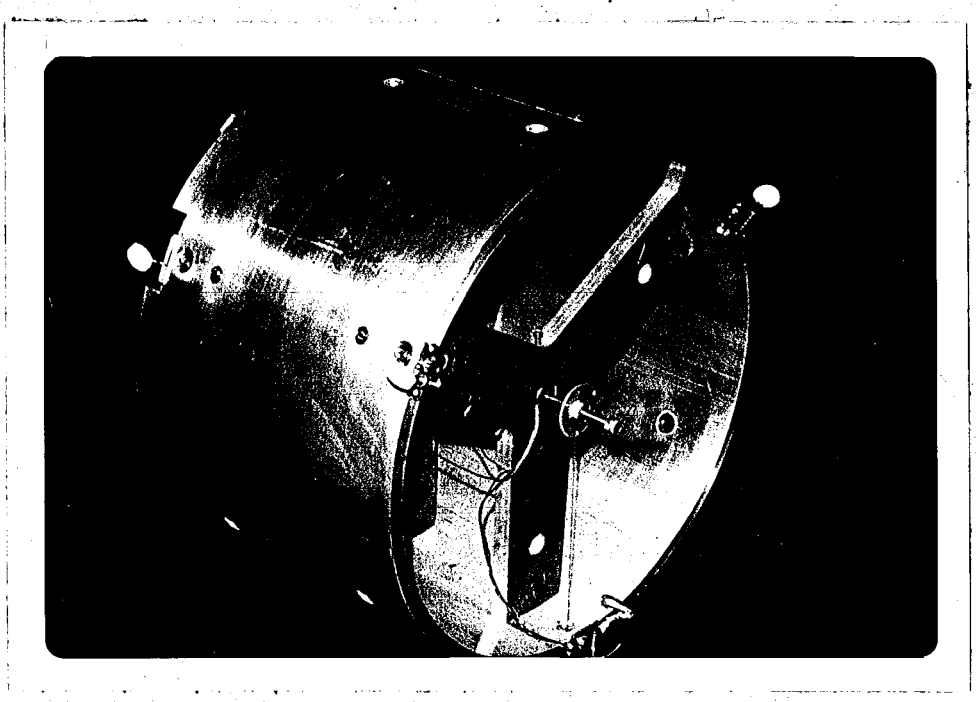

Figure 6. Photograph of Drive Unit.

another type of suspension.

In the design of this support system, consideration was given to (1) adjustability of centering, (2) low natural frequency, and (3) simplicity and ease of construction. The suspension system relies upon a triad of steel wires supporting each end of the rod. The wires are attached to the rod by an aluminum disk, which is clamped to the rod between two nuts. (This, of course, requires that the rod have external threads in the area of support.) The other end of each of the three wires is wound around the take-up drum of a single guitar key. The three guitar keys have been mounted equiangularly on the periphery at the end of the rigid aluminum cylinder, which is the basic support for the whole unit. This spider assembly is duplicated at the other end of the drum to support that end of the rod also.

The guitar keys are of the worm gear design and thus hold their position firmly. They also have a 12:1 reduction ratio, which enables a fine adjustment on the centering of the rod.

The loud speaker has the cone totally cut away to eliminate the work that it would have taken to move that large column of air. Also, the voice coil alignment spider is removed to decrease the restoring force, and thus to lower the natural frequency. Alignment of the voice coil in the magnet gap now depends upon the adjustment of the guitar keys.

The velocity transducer, Hewlett Packard model 6LV1N, is mounted in two heavy sets of spokes. These are mounted inside the aluminum cylinder, and each contains three centering bolts to allow for the centering of the transducer housing. The loud speaker magnet and the velocity transducer sensing coils are thus rigidly held together via the spokes and cylinder.

To construct this Drive Unit, the large cylinder is cut from a length of 12 inch aluminum pipe having 7/16 inch walls, and the spokes are made from 1/2 inch thick aluminum stock. The spoke material is first rough cut into two disks which are slightly larger than 12 inches in diameter and are then bolted together to the face-plate of a large lathe. These are turned down to the inside diameter of the pipe, and a 7/8 inch center hole is bored. The spokes are rough cut out of the disks with a band saw. They are then bolted together to the bed of the milling machine, and the final cuts made to each pair of the spokes. Finally, the holes for the centering bolts are drilled and tapped, and the centering bolts (6-32 x 1 1/4) inserted. Now the spokes are ready to be bolted to the cylinder with a distance of 4 1/2 inches between centers.

We now take advantage of these spokes in the process of facing the ends of the drum. A 3/4 inch rod having a center dimple on one end for dead centering is clamped in a

collet chuck used in conjunction with the face-plate. The drum with spokes is slipped over the rod, and bolts are passed through the inner set of spokes to the face-plate. Appropriate spacers are used to relieve excessive strain on the spokes. Before the bolts are tightened, the centering bolts are adjusted to give the truest turning of the drum. After facing one end of the drum, the drum assembly is reversed on the lathe, and the other end is faced. A lip is cut in this end just large enough to accept the speaker basket. The drum must have three notches cut in one end to allow the guitar keys to be recessed, such that the loud speaker basket can be mounted also. This is done by bolting the drum assembly to the milling machine bed, in the same manner as it was bolted to the face-plate of the lathe, and milling out the notches to 9/16 inch deep by 1 3/4 inches wide. The speaker is clamped to the aluminum cylinder with six bolt-down clamps made from sheet brass. The construction of the clamps is shown in Figure 7.

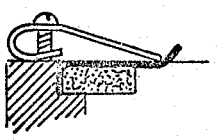

Figure 7. Construction of speaker bolt-down clamps.

The only remaining steps are drilling and tapping the holes for mounting the guitar keys and speaker clamps. The

complete assembly of the unit then follows according to Figure 5.(pg. 18)

Centering of Drive Unit

The rod of the drive unit needs to be centered before the system is used the first time. Once centered, the drive unit will remain so, but should be checked periodically if the system is to be used over a period of months. It should be checked, of course, if the system has not been used for a while.

To facilitate the centering, connect the power amplifier to the speaker and the sine wave generator (Hewlett Packard model 200CD), to the power amplifier input with gain set at minimum. The frequency of the sine wave generator should be set at ~10Hz.

There are two variables in the centering of the unit. First, there is the centering of the voice coil in the magnet gap. This is accomplished with the transducer housing left unclamped, and moving the rod manually at first to listen for rubbing. Eliminate any rubbing of the voice coil on the pole faces by adjusting the guitar keys. Do not put too much tension on the wire supports. Tension is about right if the wires give a dull ring when plucked.

Second, the transducer housing must be centered around the rod and clamped in position with its centering bolts. Careful and final adjustment here is facilitated by driving

the speaker coil sinusoidally and observing the output of the velocity transducer with the oscilloscope. (If a dual trace is available, connect one input to the power amplifier output to monitor it also.) When a good, clean output signal is obtained, the centering is complete.

After assembling and centering the complete unit, the resonant frequency was measured using an oscilloscope. The displayed transducer output indicated a natural frequency for free oscillation of 10Hz. Wire tension, however, affects this value.

CHAPTER III

DESIGN OF ASSOCIATED ELECTRONICS

In conjunction with the electromechanical drive unit, there is a system of electronic circuitry. Referring to the block diagram (Figure 8, pg. 30) of this system, we find that the reference signal generator supplies a triangular signal. This enters the summing point of operational amplifier No. 2 along with the negative, amplified transducer signal. This difference (the error signal) is amplified and fed to the voice coil to produce parabolic motion. The velocity transducer output is proportional to the velocity and after amplification in operational amplifier No. 3 is fed into the ADC input of the multichannel analyzer and to the summing point of operational amplifier No. 2 to complete the control loop.

The detector circuitry (as indicated in Figure 8, pg. 30) consists of a proportional counter with its associated high voltage power supply. The detector pulses are amplified and fed into a single channel analyzer which passes certain pulses into the coincidence input of the multichannel analyzer. Let us now consider these components.

Reference Signal Generator

The constant acceleration function is simply a square wave with a small, non-zero risetime, 2ϵ. Integration of

this function gives the velocity function--the reference signal. This triangular wave is also the form of the velocity transducer output when the drive system is operating correctly. If the velocity function were integrated, we would have the displacement function - the parabolic motion, but we do not need to generate this function as the reference signal, because it is not the dominant term in the loud speaker voltage equation.

This can be shown by considering the equations characteristic of a loud speaker[16]

$$E = L\dot{I} + RI + C\dot{x}$$
$$CI = m\ddot{x} + r\dot{x} + sx,$$

therefore

$$\dot{I} = \frac{m}{C}\dddot{x} + \frac{r}{C}\ddot{x} + \frac{s}{C}\dot{x}.$$

Combining gives

$$E = \left(\frac{Lm}{C}\right)\dddot{x} + \left(\frac{Lr}{C} + \frac{Rm}{C}\right)\ddot{x} + \left(\frac{Ls}{C} + \frac{Rr}{C} + C\right)\dot{x} + \left(\frac{Rs}{C}\right)x,$$

where the electrical and mechanical entities appearing in the coefficients are defined as:

E = driving voltage
L = inductance (electrical), coil at rest
R = resistance (electrical), coil at rest
m = natural mass of rod, coil, etc., + accession to inertia
r = mechanical resistance (force/unit velocity)

---

[16] N. W. McLachlan, Loud Speakers, (New York: Oxford University Press, 1934).

s = linear axial elastic constraint (force/unit displacement)
C = force per unit current = e.m.f. per unit velocity.

Applying the results obtained by a Fourier analysis of the acceleration (see appendix, p.69)

$$\dddot{x} = \sum_{n\,odd} \frac{4a_0}{\epsilon n\pi} \sin\frac{2n\pi\epsilon}{T} \cos\frac{2n\pi t}{T}$$

$$\ddot{x} = \sum_{n\,odd} \frac{2a_0 T}{\epsilon n^2\pi^2} \sin\frac{2n\pi\epsilon}{T} \sin\frac{2n\pi t}{T}$$

$$\dot{x} = -\sum_{n\,odd} \frac{a_0 T^2}{\epsilon n^3\pi^3} \sin\frac{2n\pi\epsilon}{T} \cos\frac{2n\pi t}{T}$$

$$x = -\sum_{n\,odd} \frac{a_0 T^3}{2\epsilon n^4\pi^4} \sin\frac{2n\pi\epsilon}{T} \sin\frac{2n\pi t}{T}$$

to this voltage equation we obtain

$$E = \left(\frac{Lm}{C}\right) \sum_{n\,odd} \frac{4a_0}{n\pi\epsilon} \sin\frac{2n\pi\epsilon}{T} \cos\frac{2n\pi t}{T}$$
$$+ \left(\frac{Lr}{C} + \frac{Rm}{C}\right) \sum_{n\,odd} \frac{2a_0 T}{n^2\pi^2\epsilon} \sin\frac{2n\pi\epsilon}{T} \sin\frac{2n\pi t}{T}$$
$$- \left(\frac{Ls}{C} + \frac{Rr}{C} + C\right) \sum_{n\,odd} \frac{a_0 T^2}{n^3\pi^3\epsilon} \sin\frac{2n\pi\epsilon}{T} \cos\frac{2n\pi t}{T}$$
$$- \left(\frac{Rs}{C}\right) \sum_{n\,odd} \frac{a_0 T^3}{2n^4\pi^4\epsilon} \sin\frac{2n\pi\epsilon}{T} \sin\frac{2n\pi t}{T}.$$

Combining like terms,

$$E = a_0 \sum_{n\,odd} \left(\frac{T}{2n\pi\epsilon}\right) \sin\frac{2n\pi\epsilon}{T} \left[\left(\left(\frac{Lm}{C}\right)\frac{8}{T} - \left(\frac{Ls}{C} + \frac{Rr}{C} + C\right)\frac{2T}{n^2\pi^2}\right)\cos\frac{2n\pi t}{T}\right.$$
$$\left. + \left(\left(\frac{Lr}{C} + \frac{Rm}{C}\right)\frac{4}{n\pi} - \left(\frac{Rs}{C}\right)\frac{T^2}{n^3\pi^3}\right)\sin\frac{2n\pi t}{T}\right].$$

The measured values of the entities are:

$L = 3.7 \times 10^{-4}$h
$R = 2.9$
$m = 6.0 \times 10^{-2}$kg
$r = 0.53$ nt/m/sec
$s = 2.5 \times 10^{2}$ nt/m
$C = 4.5$ nt/amp
$\epsilon = 2.5 \times 10^{-4}$ sec.

Upon inserting these values and using a period T = 1/10, we have

$$E = a_0 \sum_{n\,odd} \left(\frac{\sin kn}{kn}\right)\left[\left(0.395\times10^{-3} - 98.5\times10^{-3}\frac{1}{n^2}\right)\cos\frac{2n\pi t}{T} + \left(49.2\times10^{-3}\frac{1}{n} - 52.2\times10^{-3}\frac{1}{n^3}\right)\sin\frac{2n\pi t}{T}\right]$$

Where we let

$$kn = \frac{2n\pi\epsilon}{T} = 1.57\times10^{-2}\,n$$

Using the expansion of sin(kn), leads to

$$\frac{\sin kn}{kn} = 1 - \frac{(kn)^2}{3!} + \frac{(kn)^4}{5!} - \frac{(kn)^6}{7!} + \cdots$$

which will never be larger than 1 and drops about 1% for n = 15. For low n-values (i.e., first few harmonics), we can simply let it be equal to one, and expanding termwise

$$E = a_0 \sum \left[\left(-98.1\times10^{-3}\cos\frac{2\pi t}{T} - 3.0\times10^{-3}\sin\frac{2\pi t}{T}\right) \quad (n=1)\right.$$
$$+\left(-10.6\times10^{-3}\cos\frac{6\pi t}{T} + 14.5\times10^{-3}\sin\frac{6\pi t}{T}\right) \quad (n=3)$$
$$+\left(-3.54\times10^{-3}\cos\frac{10\pi t}{T} + 9.43\times10^{-3}\sin\frac{10\pi t}{T}\right) \quad (n=5)$$
$$+\left(-1.58\times10^{-3}\cos\frac{14\pi t}{T} + 6.88\times10^{-3}\sin\frac{14\pi t}{T}\right) \quad (n=7)$$
$$\left.+ \cdots\right]$$

We see that by far the largest component is

$$-98.1 \times 10^{-3} a_0 \cos \frac{2\pi t}{T} = -9.81 \times 10^{-2} a_0 \cos 62.8t$$

This is the fundamental (n=1) term corresponding to velocity, therefore the driving voltage is primarily dependent upon the velocity function.

The term

$$a_0 \frac{\sin kn}{kn} \times 0.395 \times 10^{-3} \cos \frac{2n\pi t}{T}$$

becomes the dominant term for $n \geq 125$, but its value is only $1.87 \times 10^{-4} a_0 \cos (2n\pi t/T)$, for $n = 125$, and its amplitude will be less for larger n-values. Thus, even for large n-values, no term will be larger than the velocity fundamental.

Therefore, the velocity transducer signal is subtracted from the triangular reference signal, to produce an error signal. This is then amplified and fed into the voice coil to produce the parabolic motion.

The reference signal generator indicated in Figure 8 (pg. 30) and shown schematically in Figure 9 (pg. 30), relies upon a sine wave generator (Hewlett Packard Model 200CD) for the selection of the frequency, and to provide the switching voltage. The transistor is operated as a saturated switch and thus gives out a square wave having a negative d.c. level, since this is a PNP type of transistor.

Prior to entering the first integrating operational amplifier, we must remove the d.c. level on the square wave, or else this d.c. level will also be integrated, yielding an

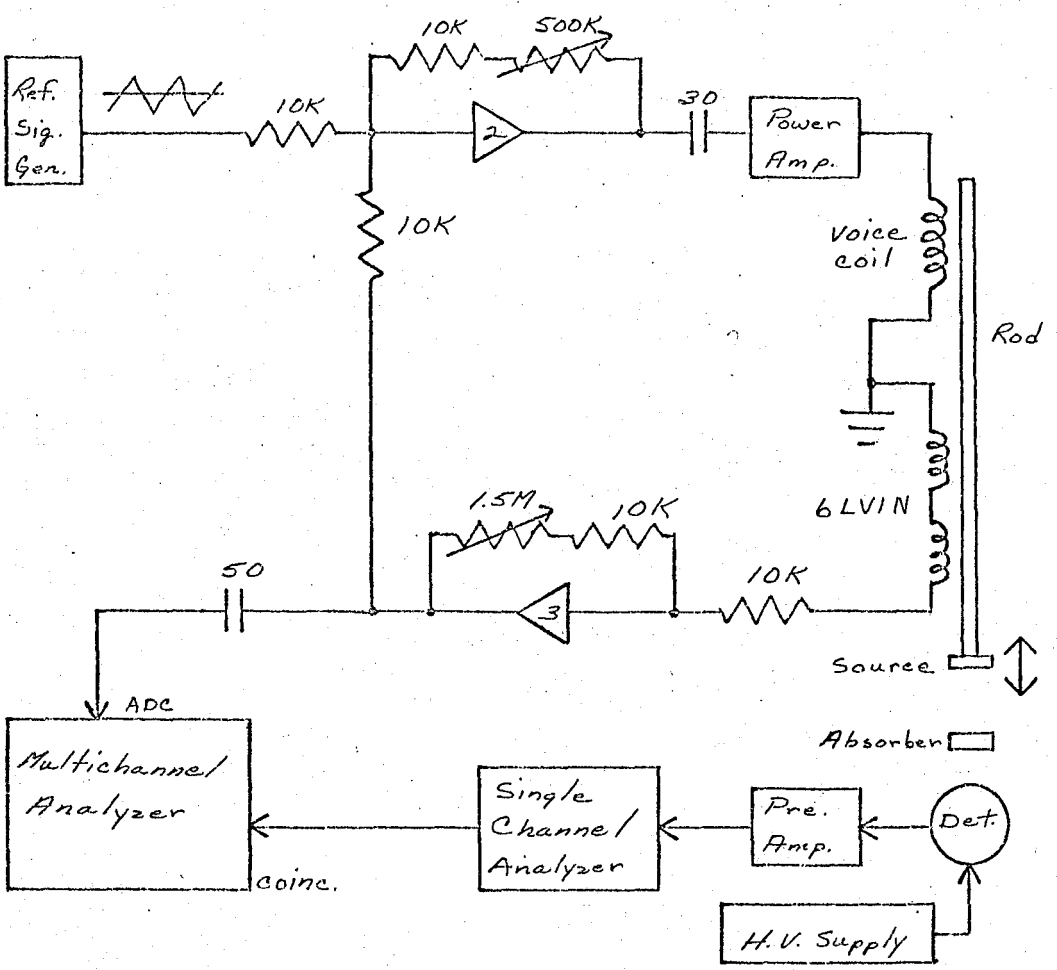

Figure 8. Block Diagram of Complete System.

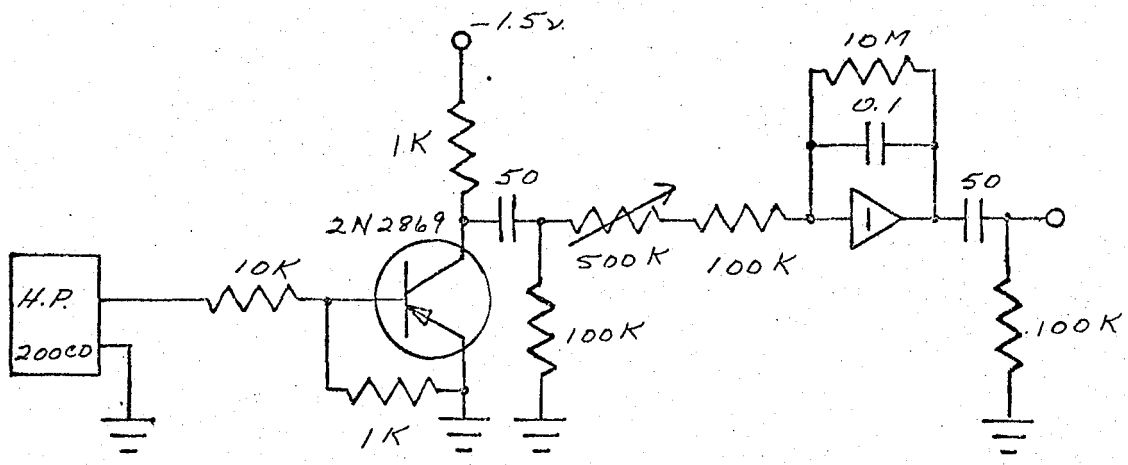

Figure 9. Reference Signal Generator.

increasing d.c. level on the output. To eliminate the d.c. level, we employ a high pass filter having a RC time constant of about 5 seconds so as not to have a large effect on the square wave. The resistance should be on the order of 100 KΩ since this is about the magnitude of the input resistance of the amplifier and thus the capacitance will be about 50 mf (non-electrolytic). At 5 hz, this will cause a voltage drop of about 2% on each half cycle. The square wave now enters the integrating amplifier and is integrated giving the triangular reference signal. We desire that this reference signal have an amplitude of 2 volts p-p, since that is the same amplitude required by the ADC input to the multichannel analyzer.

The series input resistor to the integrator is made variable so that the gain can be adjusted to give this output amplitude. This will need readjustment whenever the frequency is changed.

A similar high-pass filter (using non-electrolytic capacitors) is needed after the integrator to remove any d.c. drift from the output of this integrator.

Feedback Loop

Let us analyze the error signal amplifier and feedback loop (composed of the remaining amplifiers and transducers) as though it were a single amplifier of gain K and negative

feedback βe_o. (See Figure 10.)

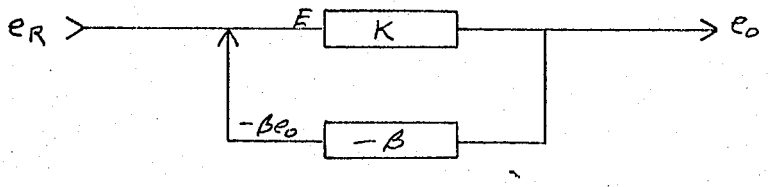

Figure 10. Amplifier with negative feedback.

With a reference signal e_R, the error signal E, which appears at input to the amplifier will be

$$E = e_R - \beta e_o$$

the output is

$$\begin{aligned} e_o &= K E \\ &= K(e_R - \beta e_o) \\ &= K e_R - \beta K e_o \end{aligned}$$

therefore

$$e_o = \frac{K}{1+\beta K} e_R$$

Returning to the error signal equation above:

$$E = e_R - \beta e_o$$

and substitution for e_o from above

$$E = e_R - \frac{\beta K}{1+\beta K} e_R = \frac{1}{1+\beta K} e_R$$

Which becomes for $\beta K \gg 1$,

$$E = \frac{1}{\beta K} e_R$$

Which means for $\beta K \gg 1$, that the error signal, the input of the error signal amplifier, is a small fraction of the reference signal. The error signal amplifier has adjustable feedback resistance to allow adjustment from unity gain up to a gain of 51.

Since the power amplifier is a D.C. amplifier, any D.C. level on the output of the error signal amplifier would be applied to the voice coil and could force the rod to one extreme or the other, or could cause a distorted motion. Therefore, the output of the error signal amplifier was coupled to the power amplifier through a 30 mf non-electrolytic capacitor, as shown in Figure 8 (pg. 30). The signal coming from the velocity transducer is of low voltage, and its relationship to the velocity is given by the manufacturer's calibration specification to be 102 mV/cm/sec. An adjustable gain amplifier is needed to amplify this transducer signal to 2 V p-p, as required by the ADC input. By incorporating this amplifier into the feedback loop, as is shown in Figure 8, any drift, which would cause a shift in the ADC register, is corrected. This amplifier then supplies both the input voltage to the ADC and the velocity signal which is to be subtracted from the reference signal to produce the error signal. The subtraction is accomplished by adding opposite polarity wave forms. In our system, βe_o is this amplified velocity signal.

This circuit arrangement thus has the advantage in that the reference signal has the same amplitude (2 v p-p) at all velocity ranges. The velocity range is determined by the gain setting of the transducer signal amplifier. In order to achieve a variety of velocity ranges, it was desirable to operate at several different frequencies. The gain of the error signal amplifier and the power amplifier are run as high as possible without going into paracytic-oscillation.

The transducer output is scoped to determine the actual velocity amplitude by using the formula

$$\text{Velocity amplitude} = \frac{V}{102\ mV} \quad \text{cm/sec.}$$

where V is the voltage amplitude in millivolts. The velocity amplitude is easily adjustable from 0.65 mm/sec to 150 mm/sec. Thus the system can be used for many types of experiments.

Each operational amplifier in this circuit has negative gain, which means that the polarity is reversed at each amplifier. This need not cause any difficulty if care is used in connecting the different components. For ease of setting up and of operation, the circuitry just described (except for the large non-electrolytic capacitor banks) was mounted into a chasis which was designed to be plugged onto the Heath Kit Operational Amplifier Model No. EUW-19A. An Operate-Balance switch was also incorporated which allows one to balance the amplifiers, and then switch immediately into the operating mode. When in the "balance" mode, all

Three of the amplifier inputs are connected to ground through their respective input resistors. Since the internal bias adjustment is sometimes not sensitive enough for the integrating amplifier (amplifier no. 1). An External-Internal bias switch and bias input jacks were added. Whenever external bias is deemed necessary, one only needs to connect the circuit shown in Figure 11 (pg. 37) to those jacks. This is about four times more sensitive than the internal bias control.

By analyzing the schematic of the multichannel analyzer (Nuclear Data, Model No. ND 110) it was determined that the ADC input (when in the Mössbauer mode) was effectively a d.c. restorer if a series input capacitor was added, and that the d.c. level was controlled by the "zero level" adjustment to some extent. We used a 50 mf electrolytic capacitor for this d.c. coupling between the final amplifier stage and the ADC input so as not to distort the wave form. With this capacitor in place the d.c. restorer was basically the circuit shown in Figure 12 (pg. 37). Where C is this coupling capacitor (also shown in Figure 8, pg. 30), and R_L is the input resistance of the analyzer (approximately 70 K Ω).

The ADC requires that the velocity signal be 2 volts p-p with an offset of -1 volt d.c. This d.c. restorer accomplished this very nicely.

The power amplifier, a two-stage complimentary symmetry

circuit, was based on a design given by R. L. Cohen, et.al.,[17] and by G. K. Wertheim.[18] However, different output transistors were chosen on the basis of reduced cost and availability. The circuit shown in Figure 13 (pg. 37) was used. The voltage supplies were four six-volt storage batteries connected in series with the center tap as ground. This gave a very stable D.C. power source even with the battery charger on, which was necessary due to the long periods of operation.

Detector Circuitry

The detector is a Reuter-Stokes proportional counter (Model No. RSG-30A). This particular detector requires about 2000 volts D.C. for operation. The gain of the proportional counter is very sensitive to fluctuations of high voltage, therefore the power supply must be well regulated.

The basic power supply uses a half-wave rectifier with two R.C. filters followed by a series of gas voltage-regulator tubes (See Figure 14, pg. 38). The no-load voltage at the output of the filters was about 6000 volts. Under a load of 8 mA this output voltage dropped to 4000 volts.

---

[17] R. L. Cohen, P. G. McMullin, G. K. Wertheim, "High Velocity Drive for Mössbauer Experiments," Rev. Sci. Inst. 34, No. 7 (1963), p. 671-673.

[18] Gunther K. Wertheim, Mössbauer Effect: Principles and Applications (New York: Academic Press, 1964), p. 22.

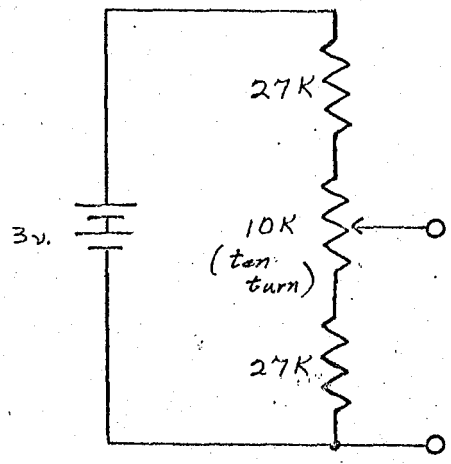

Figure 11. External Bias Source.

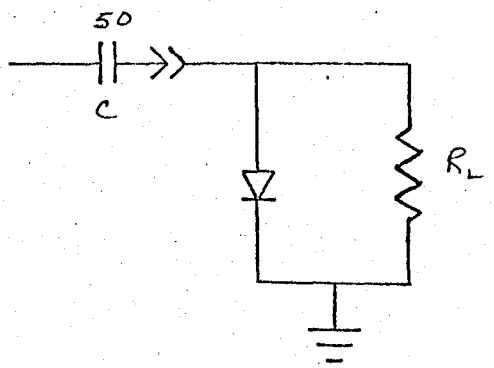

Figure 12. Effective D.C. Restorer at ADC Input.

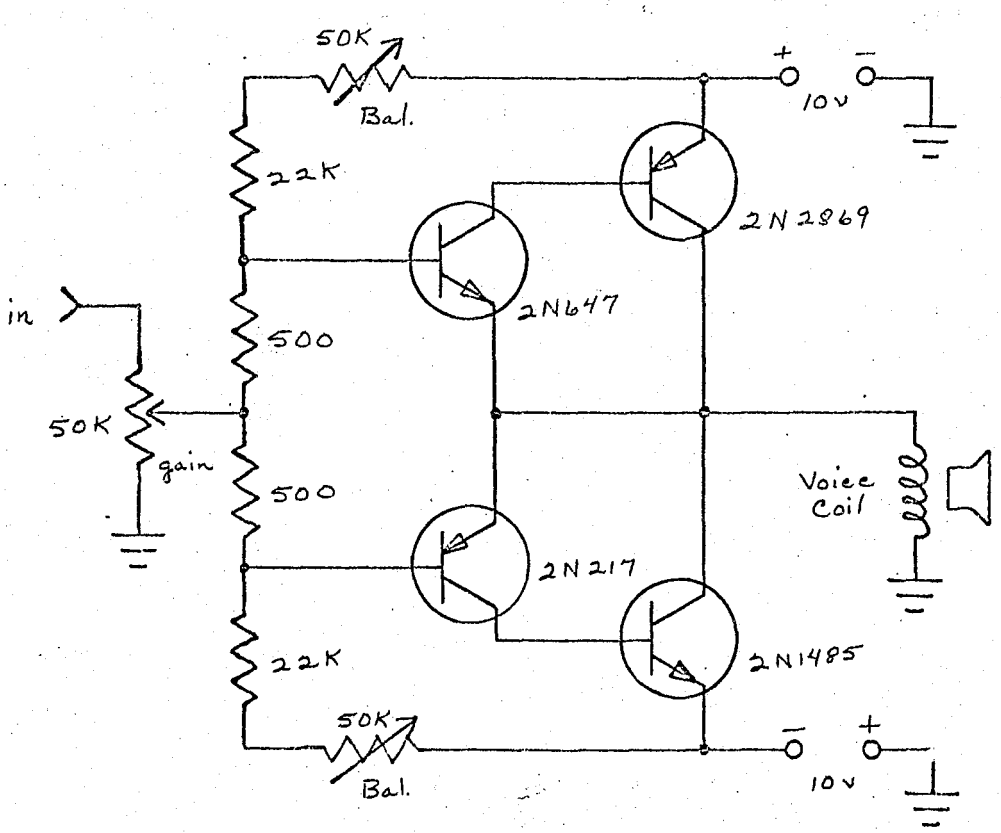

Figure 13. Power Amplifier.

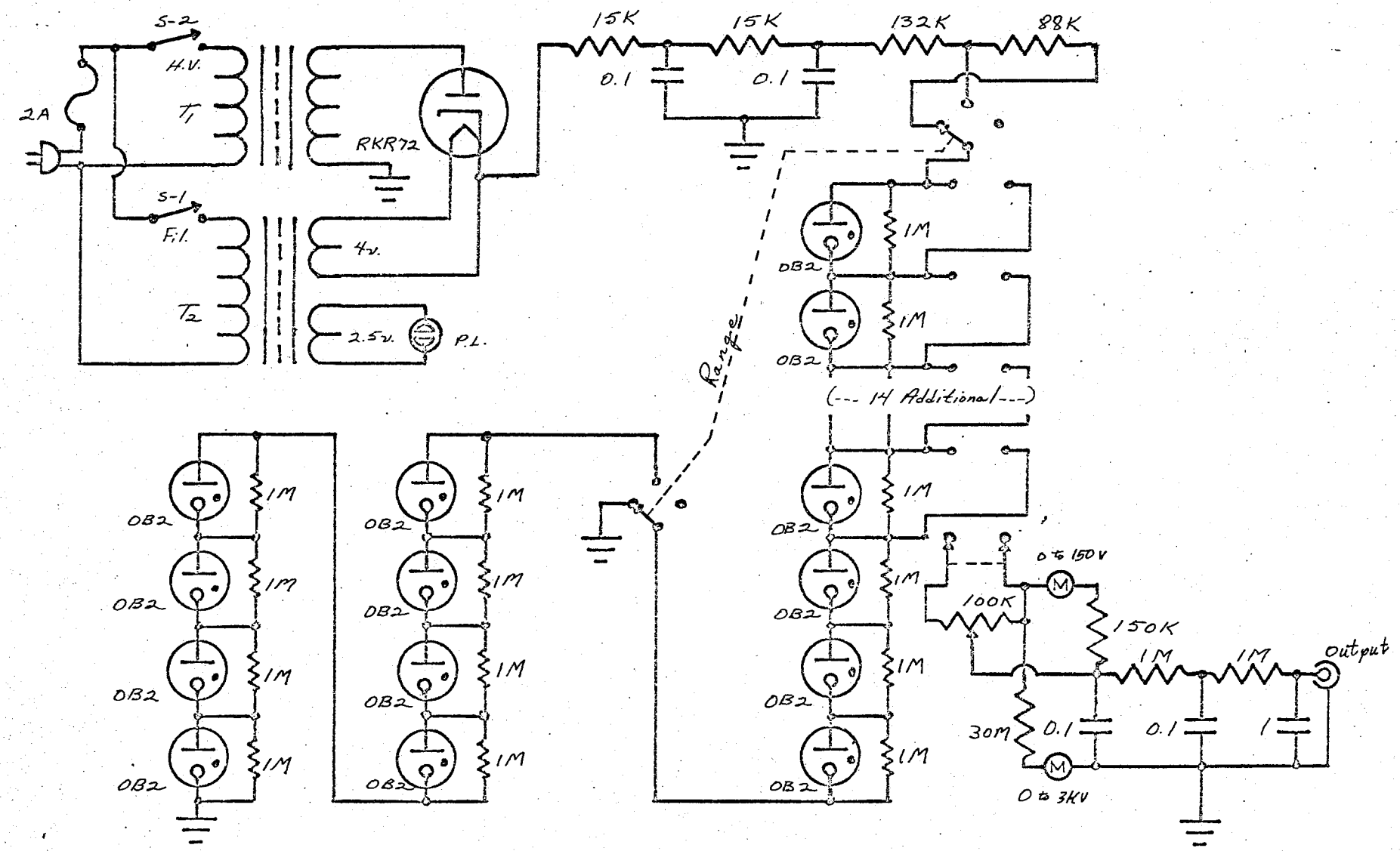

Figure 14. High Voltage Power Supply (330-3000 volts).

Since the minimum current needed for regulation by an OB2 is 5 mA, this will allow 3 mA that can be drawn by the switching and metering circuit and the external load and still maintain regulation. Since twenty OB2's in series will regulate 2200 volts, that leaves 1800 volts at 8 mA to be handled by the series resistor. It was decided to use ten 22 KΩ, 2 watt resistors in series to handle this power.

To extend the usefulness of this power supply, an additional eight OB2's can be switched into the lower end of the earlier string of twenty; at the same time, the switch cuts out four of the 22 KΩ voltage dropping resistors leaving only 132 KΩ. This then still allows about 8 mA to flow through the VR tubes for regulation. The total of 28 VR tubes extends the regulated output voltage to 3000 volts D.C.

An eighteen position, two wafer rotary switch is used as a course adjustment to select the output voltage with one position used as an "off" position. A 100 KΩ potentiometer is used as a fine adjustment. The effect of this switching arrangement is to switch across each of the upper seventeen OB2's in sequence with the course adjustment. The fine adjustment then is used to give a smooth adjustment to any voltage as found across that selected tube. The two ranges of output voltages are 330 to 2200 volts and 1200 to 3000 volts.

After this voltage selector come the meters and some

final R-C filters as shown. This particular arrangement gave very smooth output to the detector.

The charge-sensitive preamplifier, Figure 15 (pg. 41), was designed and built by Fred W. Inman. It amplifies the detector pulses and delivers positive output pulses whose voltage amplitudes are proportional to the energy of the detected gamma rays. The B+ (250 volts) for this circuit is supplied by the Hewlett Packard power supply (Model 721-B), and the fillaments, needing a very stable 6 volts, are powered by one of the storage batteries. The output of this amplifier is connected to the input of the single channel analyzer, (Figure 16 (pg. 42).

As a pulse enters the single channel analyzer it is applied simultaneously to two amplitude discriminators (Schmidt circuits). The triggering level of the lower level discriminator is adjusted so that any pulse corresponding to energy less than 14.4 kev will not trigger it. The other, the upper level discriminator, is adjusted such that it is triggered only when a pulse comes whose energy is greater than the 14.4 kev. Thus a pulse corresponding to 14.4 Kev will trigger the lower level discriminator, but will not trigger the upper level discriminator. Also, any pulse whose energy is greater than the 14.4 kev will trigger both discriminators. With the output of these two discriminators

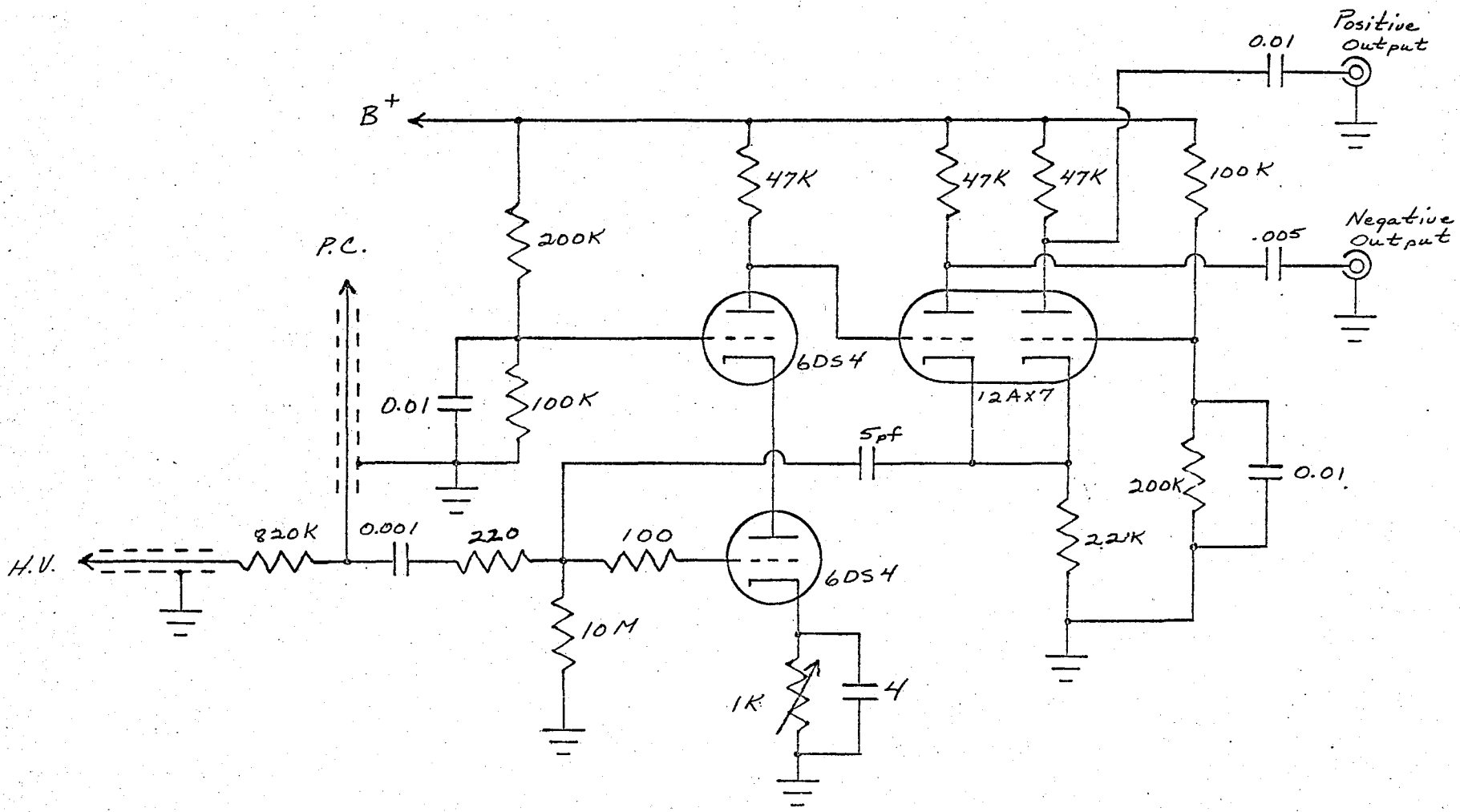

Figure 15. Charge Sensitive Preamplifier.

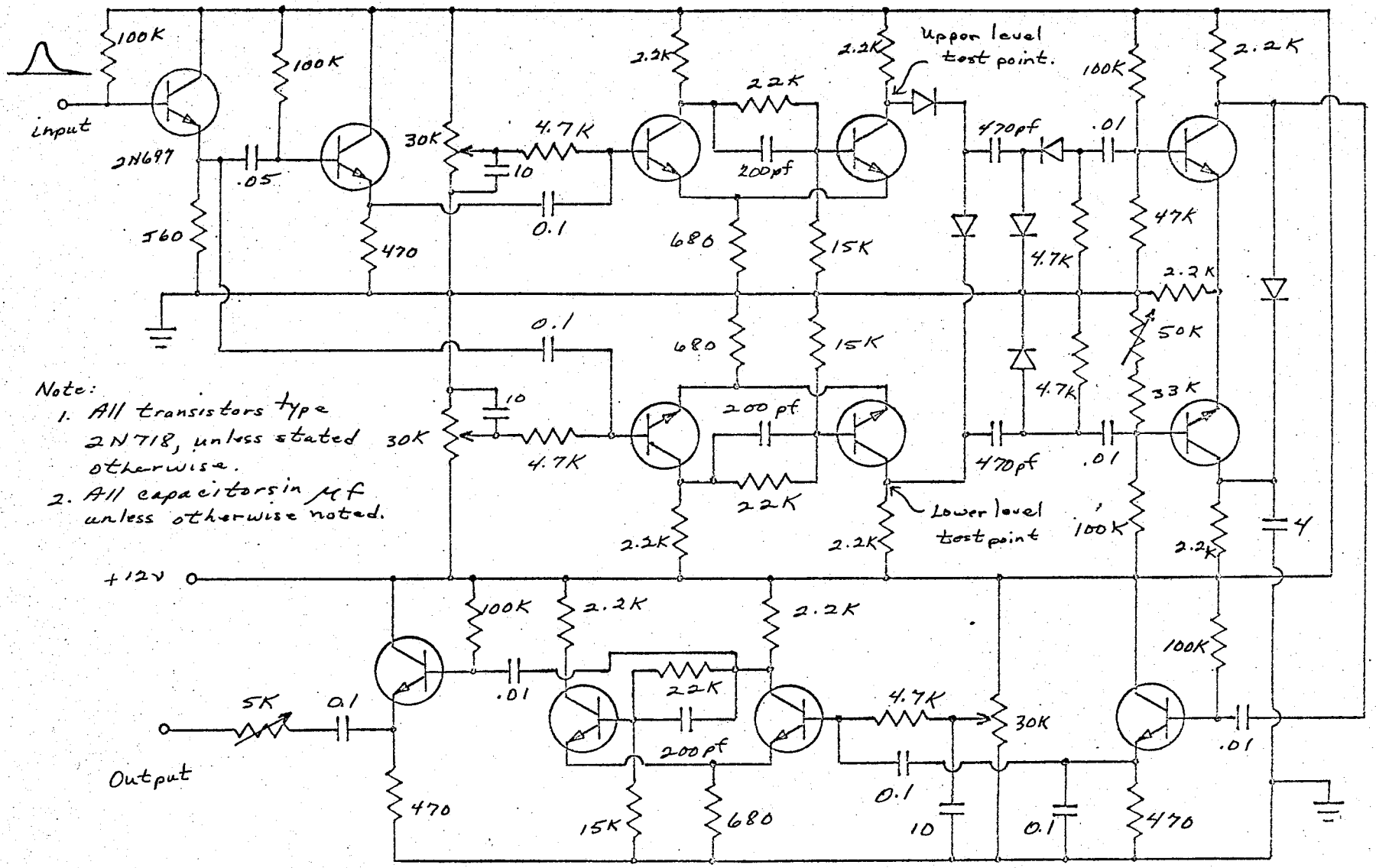

Figure 16. Single Channel Analyzer.

fed into an anticoincidence circuit,[19] there is a resulting pulse only when the lower level is triggered and the upper level is not (i.e., only when a 14.4 kev pulse is detected will there be an output pulse). This output pulse is fed via an emitter follower into another Schmidt circuit to give a more uniform output pulse shape which is connected through another emitter follower to the coincidence input of the multichannel analyzer.

Whenever a pulse arrives at the coincidence input of the multichannel analyzer, the analyzer stores one count in the channel corresponding to the velocity signal appearing at the ADC input at that instant. By this means we tally counts to give the absorption spectrum in which a drop in intensity indicates a velocity corresponding to resonant absorption.

---

[19] Robert L. Chase, Nuclear Pulse Spectrometry, (New York: McGraw-Hill, Inc., 1961), p. 64.

CHAPTER IV

BALANCE AND OPERATION OF CONSOLIDATED APPARATUS

Balance and Operation of System

Now that each of the components of the electro-mechanical drive system has been described in detail, let us consider the consolidated system. Each component has certain adjustments to be made to enable it to operate properly for better than twelve hours. Some of these adjustments are made before the components are connected into the system, others are made afterwards.

This chapter will be concerned with the adjustments that have to be made on the entire system in order for it to operate properly. This will necessitate returning to some previously discussed components (e.g., all of the adjustments and hooking up of a single component will not be completely discussed at one time). This will be especially noticed in the discussions of the function generator, the adjustment and operation of which is most critical.

Due to the need of stability and of careful adjustments to be made, the Heath Kit operational amplifier should be plugged in and turned on first. The function generator module which plugs onto the front of this instrument should be left off, until the B+ supplies have been adjusted according to the manufacturer's specifications. A warm-up period of at least

one half hour is recommended before attempting this adjustment. Too short a warm-up period will result in D.C. drift in the operational amplifiers.

While the amplifier warms up, we turn our attention to the balancing of the power amplifier. Connect the power amplifier to the storage batteries or some other well filtered source supplying ± 10 to ± 12 volts at about 2 amps. Then with the input open and the gain control at maximum, measure the no-load output with a sensitive VTVM or DC oscilloscope. Adjust the balance controls until zero output voltage is obtained at all settings of the gain control. This completes the balancing of the power amplifier. Also check the centering of the drive unit according to Chapter 2.

Now return to the operational amplifiers, and balance the B+ supplies according to specifications. Then plug the function generator module onto the amplifier bank and place the Operate-Balance switch in the "Balance" position. With the amplifier's D.C. power switch "On", adjust the bias settings of each amplifier using a very sensitive VTVM, or better yet, use the oscilloscope on its most sensitive D.C. range. Adjust to zero output at each amplifier (test points are supplied) with its gain setting adjusted as high as is practical. Recheck each amplifier several times. If external bias is deemed necessary for the first amplifier, simply connect the circuit shown in Figure 11 (pg. 37) to the bias

input jacks provided, and switch to "external bias".

Leave the function generator in the "balance" mode and connect the associated driver circuitry as shown in Figure 8 (pg. 30). Adjust the audio oscillator for frequency and for maximum output, and check the output of the square wave generator for a clean, sharp wave form by using the oscilloscope.

Again, check the amplifier outputs to see if there has been excessive drift during the intervening moments. (Some drift will be inevitable.) If the drift has not been excessive, turn down the gain controls of the amplifiers and switch to the "Operate" mode. If the speaker begins to vibrate wildly, due to the feedback signal being in phase with the reference signal, reverse its leads. Connect the oscilloscope to the output of the first amplifier, and adjust its gain until the resulting triangle wave is 2 V p-p. This sets the reference signal. Next set the power amplifier gain at maximum and adjust the gain controls of the other two amplifiers until a good, sharp triangular wave having an amplitude corresponding to the desired velocity range is obtained from the transducer output. When the wave form thus obtained is sharp, the output of the third amplifier should be a 2 V p-p triangular wave. If a high frequency oscillation occures while trying to make these adjustments, there is too much gain in the feedback loop.

Once this part of the system is adjusted properly, turn

down the power amplifier gain to zero, and connect the oscilloscope to the transducer output and gently pull on the end of the rod. If the transducer output is positive with respect to ground as the rod moves outward, the information stored in the higher numbered channels corresponds to a positive velocity and the lower channel numbers to a negative velocity.

Also, while the unit is still, attach the Mössbauer source material to the end of the rod. The power amplifier gain can then be returned to its maximum setting. Place sufficient shield material (sheet lead) around the driver unit for protection. Also line up the collimator (1/2 inch thick lead plate with a 1/4 inch hole through it) and place the detector behind it, aligning the entrance window with the hole in the plate.

Connect the detector to the charge sensitive preamplifier, connect the preamplifier to the high voltage power supply, and connect the oscilloscope to the output of the preamplifier. Turn the high voltage to about 2000 volts, and observe the detector pulses on the oscilloscope. Adjust the cathode bias potentiometer of the preamplifier until the best shaped pulses are obtained.

Next connect the single channel analyzer to the 12 volt d.c. supply. (The positive half of the series of storage batteries makes a very good source, but be careful to make proper connections.) Also, connect the positive output of

the preamplifier to the input of the single channel analyzer, and connect the trigger input of the oscilloscope to the lower discriminator output (e.g., test point). Switch to triggered sweep and observe the detector pulses as the lower discriminator level is adjusted to that level such that the 14.4 kev gamma pulses (for Fe^{57}) are still seen on the oscilloscope.

Now connect the trigger input to the upper discriminator output, and adjust that level until only pulses greater than 14.4 kev are seen.

To help determine which pulses are the 14.4 kev gamma pulses, use one of the Mössbauer absorbers. By placing the absorber over the collimator hole (on the source side), the 14.4 kev gamma rays will be noticeably attenuated, whereas the 123 kev gammas will be very slightly attenuated. These two spectral lines are, however, superimposed upon a line of 6 kev X-rays and a continuous band of thermal noise which complicates the situation.

Now that we have the upper and lower discriminators set, we can check the operation of the anticoincidence output. We should only see pulses corresponding to the 14.4 kev gamma rays on the oscilloscope.

There are two other adjustments to be made on this single channel analyzer. To balance the anticoincidence circuitry, the 50 K Ω rheostat is adjusted to give the best output pulse

from that part of the circuit. The second adjustment (30 K Ω potentiometer) is to set the bias level of a Schmidt circuit used as a pulse shaping circuit. If it is not adjusted properly, no pulses will be seen at the output of the single channel analyzer. Connect the output of the single channel analyzer to the "coincidence input" of the multichannel analyzer.

There remains only one more connection to be made. That is to connect the output of the third amplifier of the function generator to the ADC input of the multichannel analyzer. This applies the amplified transducer output to the ADC input. Set the zero level adjustment on the analyzer to minimum and switch to "Mössbauer" mode.

Our system is now complete and all adjustments have been made. We are ready to take a spectrum. Tape or by some other means attach one of the Mossbauer absorbers over the collimator hole on the source side, and start the analyzer. Allow the system to run undisturbed until sufficient counts have accumulated.

CHAPTER V

EXPERIMENTAL DATA

Read-out Methods

There are several methods of observing or obtaining the information (spectrum) stored in the analyzer. First, the spectrum can be displayed on the oscilloscope. This is not very quantitative, but is of value in checking progress periodically during a "run". Second, the stored information can be fed into a strip-chart recorder, thus giving a permanent display similar to that on the oscilloscope, but this also is not too quantitative because the resonant absorption will be 20% or less.

Thus, a method to read out the actual count total in each channel is needed, from which data a graph can be made. The Nuclear Data analyzer can be equipped with typewriter output, which automatically types out the total for each channel. At the time this research was done, our analyzer was not so equipped, however, this capability was added later.

To satisfy the need at the time, a device was designed and built by Fred W. Inman. The circuit, Figure 17, consists of a unijunction transistor relaxation oscillator, which sends pulses to the analyzer's "digital advance" input. Each pulse causes the analyzer to set the level of binary outputs cor-

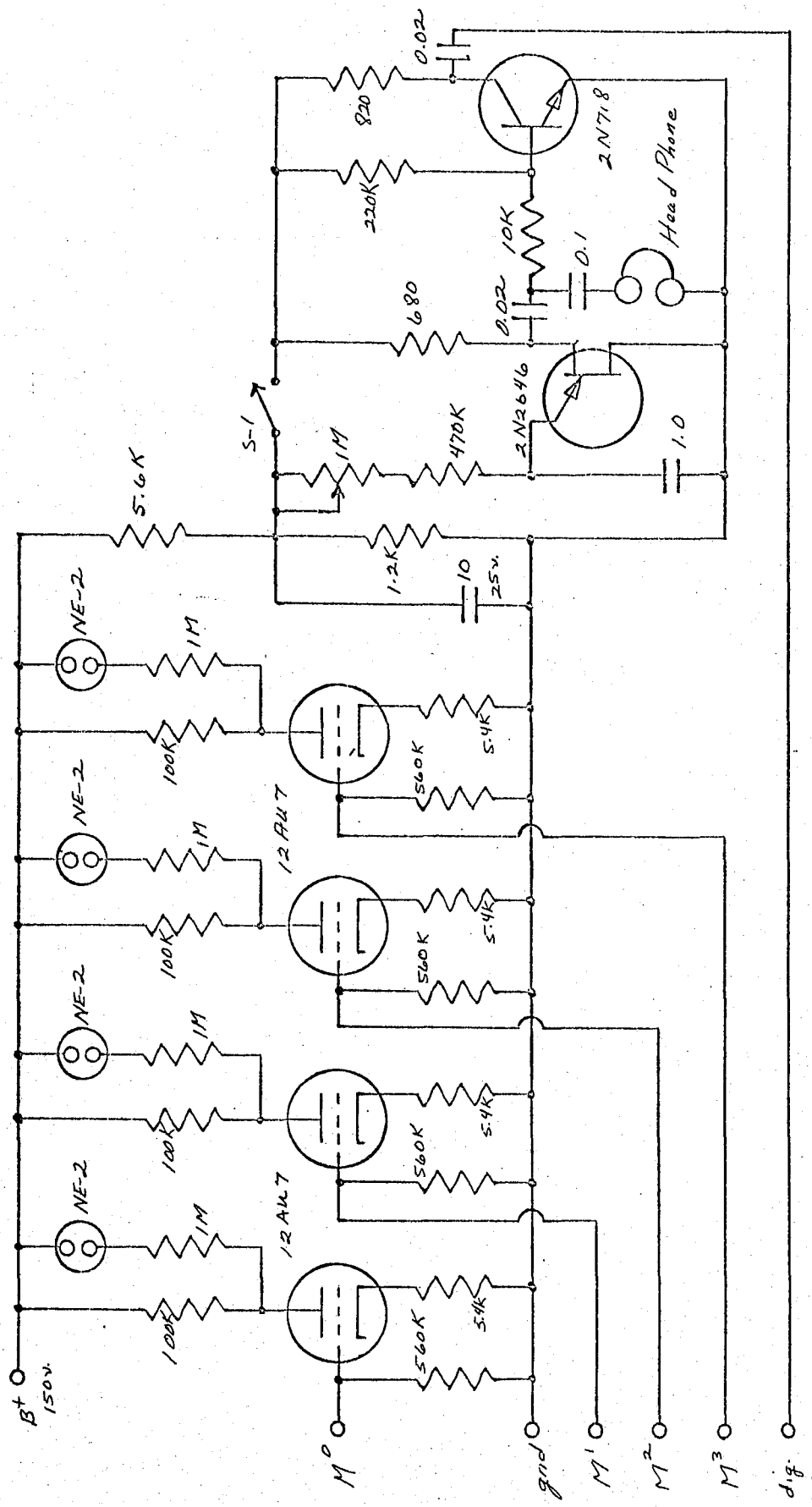

Figure 17. Read-out Module.

responding to the first digit. The next pulse will trigger the feed out of the next digit, and so on for the five digits in the number of counts in the first channel. This will be followed by three "zero" pulses, and then the five digits in the number of counts in the second channel, again three "zero" pulses, and so forth for each of the 128 channels. The first channel is the clock. Its data is of no value to us.

These four binary outputs constitute a BCD digit and are fed into a series of four neon indicator lamp drivers, a most simple and effective BCD display. In the plate circuit of each triod is a neon glow tube to indicate the level of the binary signal. The first neon bulb is assigned the value "1", the second is assigned the value "2", the third "4", and the fourth "8". To determine the value of each digit, one merely adds the values corresponding to the glowing bulbs.

A headset is used to hear the click of the oscillator pulse and thus know that the next digit is ready for tabulation. The frequency of the oscillator is adjustable so that an individual can set his own pace, or even turn it off at any spot, and start again from that same place. After some practice, one can read out the total storage in about 30 minutes - that's one digit every two seconds. This is admittedly a slow and tedious process, but the best available at that time.

Samples of Data

The system has been used to obtain the three types of spectra. Table I (pg. 54) and its graph, Figure 18 (pg. 55), is a spectrum of the isomer shift showing the percent absorption. The velocity amplitude was 0.65 mm/sec for this spectrum. Table II (pg. 56) and its graph, Figure 19 (pg.57), is a spectrum showing the magnetic hyperfine structure, where the velocity amplitude was set at 10 mm/sec. For these two spectra the velocity scale was not calibrated, but the spectra are rather clear. The spectra of $FeCl_2$ which shows quadrupole splitting, Table III (pg. 58), was made by John Roscelli as an advanced laboratory project. He calibrated the velocity scale by taking a hyperfine structure spectrum of Fe_2O_3, and comparing it with a published spectrum.[20] Table IV summarizes his velocity calibration. A graph of his quadrupole coupling spectrum is presented in Figure 20, (pg.59)

TABLE IV

VELOCITY CALIBRATION
FOR FIGURE 20

Channel Number	Velocity (mm/sec)
16	-8.0
30	-4.2
69	5.6
81	8.8

[20]Gunther K. Wertheim. Mössbauer Effect: Principles and Applications. New York: Academic Press, 1964. p. 78.

TABLE I

ISOMER SHIFT
STAINLESS STEEL ABSORBER

Channel Number	Counts	Channel Number	Counts	Channel Number	Counts
1	9998	41	9396	81	9488
2	9605	42	9435	82	9557
3	9619	43	9336	83	9585
4	9542	44	9331	84	9485
5	9314	45	9146	85	9584
6	9611	46	9191	86	9505
7	9394	47	9207	87	9651
8	9660	48	9185	88	9708
9	9642	49	9015	89	9694
10	9334	50	9042	90	9695
11	9520	51	9002	91	9794
12	9344	52	8837	92	9707
13	9263	53	8708	93	9669
14	9428	54	8549	94	9955
15	9365	55	8422	95	9735
16	9440	56	8372	96	9993
17	9537	57	8337	97	9851
18	9618	58	8186	98	9957
19	9430	59	7971	99	10008
20	9482	60	7975	100	9941
21	9545	61	7845	101	9914
22	9330	62	7774	102	9814
23	9375	63	7769	103	9996
24	9410	64	7655	104	9904
25	9544	65	7715	105	9786
26	9346	66	7787	106	10005
27	9633	67	7810	107	10192
28	9291	68	8030	108	9619
29	9273	69	8055	109	4029
30	9378	70	8275	110	1539
31	9177	71	8544	111	1005
32	9422	72	8505	112	529
33	9435	73	8786	113	71
34	9529	74	8880	114	4
35	9331	75	8901	115	4
36	9337	76	8991		
37	9348	77	8919		
38	9386	78	9164		
39	9371	79	9294		
40	9251	80	9512		

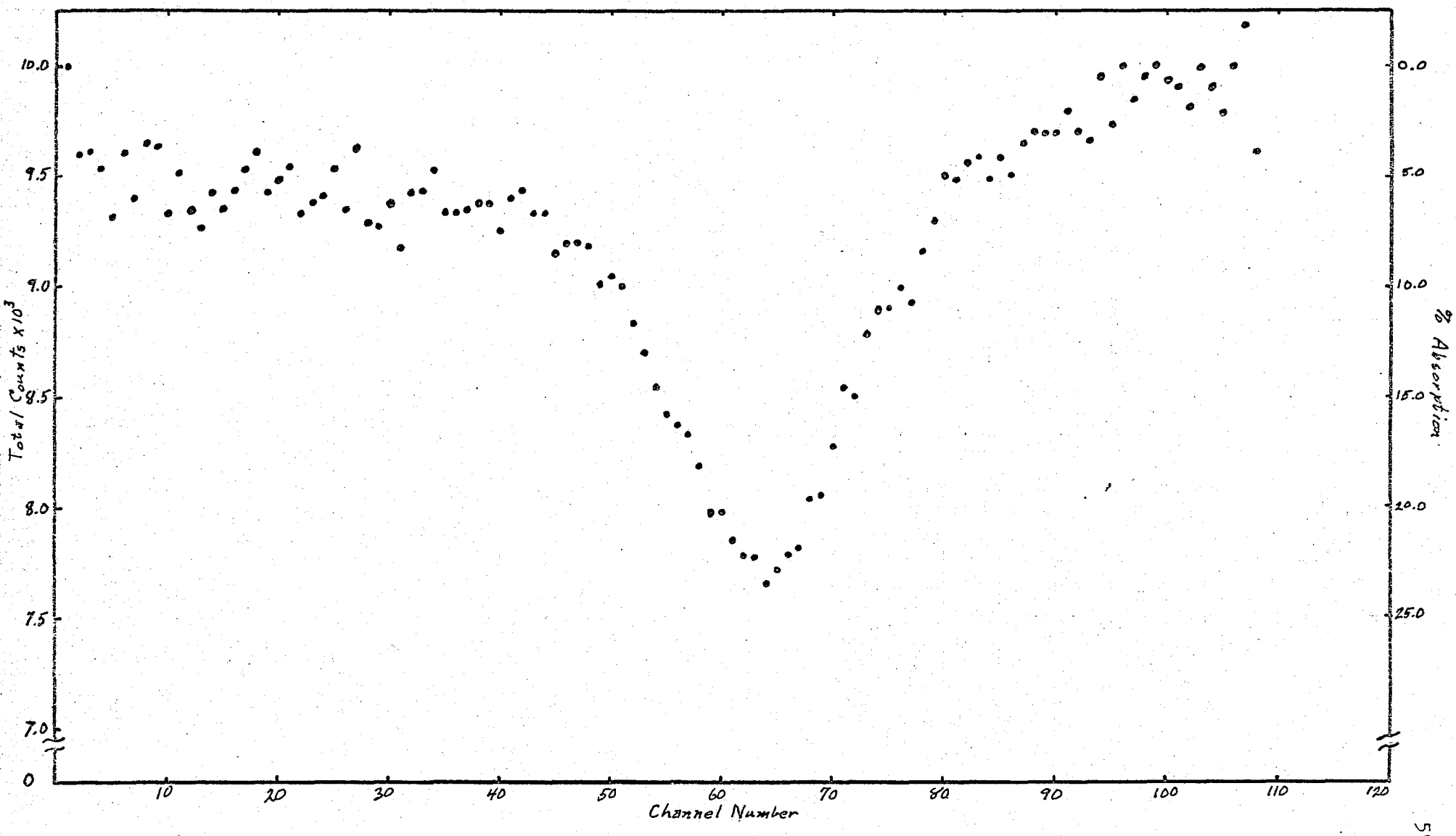

Figure 18. Isomer Shift Mössbauer Spectrum. Stainless Steel vs Pt:Co^{57}.

TABLE II

MAGNETIC HYPERFINE STRUCTURE
NATURAL IRON ABSORBER

Channel Number	Counts	Channel Number	Counts	Channel Number	Counts
1	9256	41	9025	81	9183
2	9148	42	8836	82	9377
3	9201	43	9105	83	9435
4	9128	44	9202	84	9318
5	8990	45	9103	85	9348
6	9076	46	9096	86	9610
7	9127	47	9183	87	9659
8	9009	48	8819	88	9486
9	9149	49	8893	89	9480
10	9183	50	9016	90	9469
11	8974	51	8963	91	9552
12	9026	52	9130	92	9228
13	9184	53	9074	93	9344
14	9227	54	9083	94	9133
15	9053	55	8949	95	9265
16	9043	56	8896	96	9304
17	9132	57	9003	97	9211
18	9211	58	8783	98	9206
19	9208	59	8970	99	9214
20	9200	60	9183	100	9158
21	9017	61	9102	101	9272
22	9177	62	9088	102	9235
23	9217	63	9328	103	9313
24	9080	64	9193	104	9240
25	8949	65	9172	105	9226
26	8770	66	9023	106	9390
27	8633	67	8936	107	9322
28	8641	68	8740	108	9609
29	8828	69	8795	109	9464
30	8794	70	9088	110	9491
31	9117	71	9233	111	9542
32	8964	72	9199	112	9454
33	9055	73	9302	113	9582
34	8994	74	9296	114	9528
35	9046	75	9552	115	9580
36	8997	76	9284	116	9456
37	8785	77	8977	117	9363
38	8560	78	8762	118	9623
39	8760	79	8897	119	9368
40	8597	80	8891	120	9473

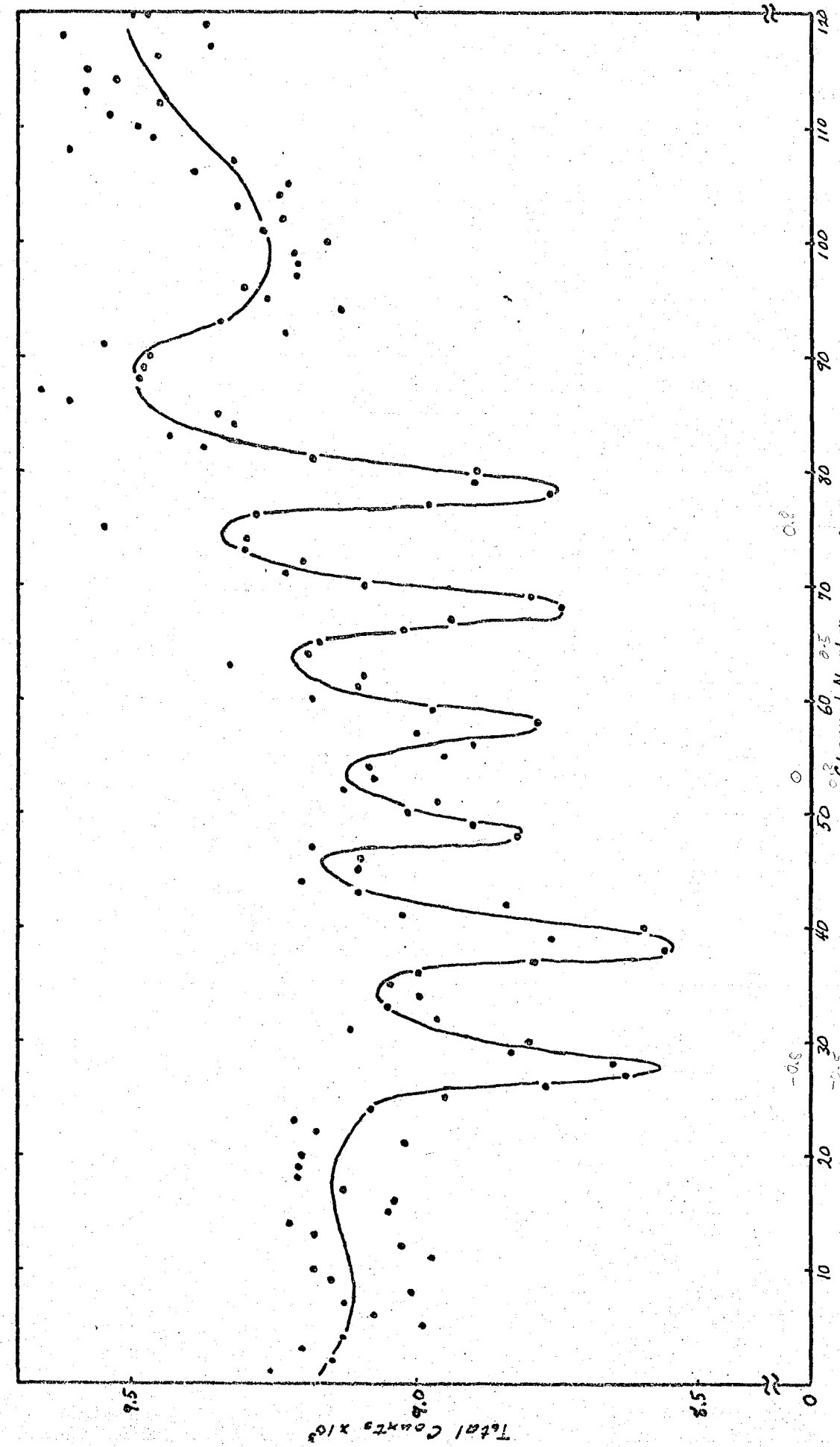

Figure 19. Magnetic Hyperfine Mössbauer Spectrum for Natural Iron.

TABLE III

QUADRUPOLE COUPLING
$FeCl_2$ ABSORBER

Channel Number	Counts	Channel Number	Counts	Channel Number	Counts
1	76044	41	70195	81	71903
2	83991	42	73352	82	73891
3	79984	43	69935	83	74138
4	78361	44	66234	84	74439
5	74881	45	66117	85	74091
6	72824	46	67158	86	73512
7	70498	47	65839	87	71878
8	72801	48	67840	88	73045
9	72945	49	69033	89	74027
10	74475	50	69814	90	74003
11	76240	51	69251	91	73716
12	76254	52	70528	92	75394
13	75301	53	70427	93	73822
14	75936	54	72950	94	74174
15	74849	55	68268	95	75316
16	74151	56	68963	96	75127
17	73784	57	66468	97	74179
18	73753	58	68220	98	75871
19	74457	59	68716	99	77562
20	72489	60	69878	100	76139
21	72662	61	70846	101	74899
22	73019	62	72324	102	75982
23	72926	63	71950	103	76317
24	72806	64	73158	104	76810
25	73126	65	71263	105	74847
26	73120	66	71912	106	81703
27	73710	67	73635	107	83210
28	72862	68	73652	108	73461
29	72190	69	71427	109	40908
30	72394	70	72308	110	16156
31	71129	71	72487	111	53058
32	71173	72	73155	112	33813
33	70028	73	73069	113	35835
34	72977	74	72866	114	15010
35	70984	75	72166	115	69
36	70864	76	72290		
37	70593	77	72747		
38	72059	78	73507		
39	70343	79	72959		
40	72576	80	72699		

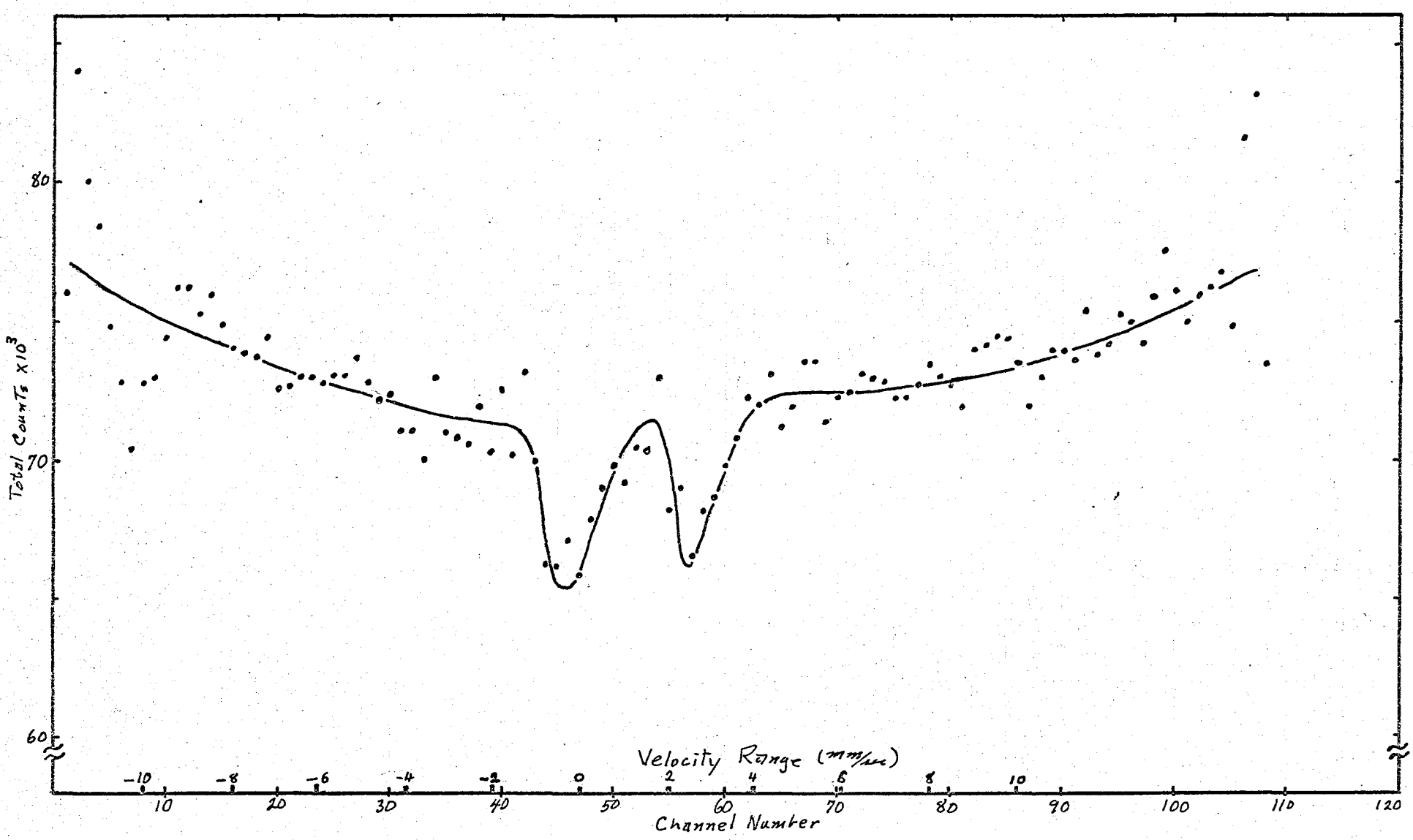

Figure 20. Quadrupole Coupling Mössbauer Spectrum for $FeCl_2$.

CHAPTER VI

CONCLUSION

This project, which was of an engineering nature, was to build a Mössbauer Drive System to be used for classroom demonstration, and as a tool for upper division or graduate research. The results obtained using this drive system are clear and show a very pronounced drop at points of resonance.

The centering of the drive unit is easily accomplished and has good stability. The unit is capable of a larger range of velocity amplitudes than was expected. At any given amplitude, it operates with very good linearity. Little or no difficulty was encountered with this particular drive unit design.

When working with the entire system it is essential that each part be carefully balanced to provide proper operation during the many hours that are necessary to tally sufficient counts. Balance is especially critical in the operational amplifiers to minimize drift, and produce a flat nonabsorption spectrum. In the spectrum taken by John Roscelli, Figure 20 (pg. 59); it appears from the sloping nonabsorption regions that the system was not adjusted for good linearity.

In the single channel analyzer, adjustment of the window-width to allow only a narrow peak, containing the 14.4 kev

gamma pulses, leads to better spectrums in that there will be less spurious counts and thus the per cent absorption will be greater.

In general, the complete system was found to operate in a very satisfactory manner with a minimum of difficulties.

BIBLIOGRAPHY

BIBLIOGRAPHY

A. BOOKS

Chase, Robert L. Nuclear Pulse Spectrometry. New York: Mc Graw-Hill, 1961.

Clark, George L. (ed). The Encyclopedia of Spectroscopy. New York: Reinhold Publishing Corporation, 1960.

Compton, D.M., A.H. Schoen. The Mössbauer Effect. New York: John Wiley & Sons, Inc., 1962.

Das, T.P., E.L. Hahn. Nuclear Quadrupole Resonance Spectroscopy. New York: Academic Press, 1958.

DeBenedetti, Sergio. Nuclear Interactions. New York: John Wiley & Sons, Inc., 1966.

Frauenfelder, Hans. The Mössbauer Effect, a Review with a Collection of Reprints. New York: W. A. Benjamin, Inc., 1962.

French, A.P. Special Relativity. New York: W.W. Norton & Co., Inc., 1966.

Gol'danskii, V.I. The Mössbauer Effect and its Applications to Chemistry. New York: Consultants Bureau, 1964.

Gruverman, Irwin J. (ed). Mössbauer Effect Methodology. 4 Vols. New York: Plenum Press, 1968.

Howard, Robert A. Nuclear Physics. Belmont: Wadsworth Publishing Company, Inc., 1963.

Matthias, E., D.A. Shirley (ed). Hyperfine Structure and Nuclear Radiations. New York: John Wiley & Sons, Inc., 1968.

McLachlan, N.W. Loud Speakers. New York: Oxford University Press, 1934.

Melissinos, Andrian C. Experiments in Modern Physics. New York: Academic Press, 1966.

Mössbauer Effect Selected Reprints. Published for the AAPT Committee. New York: American Institute of Physics, 1964.

Muir, Arthur H., Ken J. Ando, Helen M. Coogan. Mössbauer Effect Data Index 1958-1965. New York: Interscience Publishers, 1966.

Resnick, Robert. Introduction to Special Relativity. New York: John Wiley & Sons, Inc., 1968.

Segre, Emilio. Nuclei and Particles. New York: W.A. Benjamin, Inc., 1964.

Stone, John M. Radiation and Optics. New York: McGraw-Hill Co., Inc., 1963.

Wertheim, Gunther K. Mössbauer Effect: Principles and Applications. New York: Academic Press, 1964.

B. PERIODICALS

Adler, Alan D., Michael Home. "A Simple Mössbauer Effect Apparatus," Am. J. Phys. 34, No. 3, 189 (1966).

Artem'ev, A.N., G.V. Smirnov, E.P. Stepanov. "Investigation of the Mössbauer Spectrum of Resonantly- Scattered Nuclear Radiation of Fe^{57}," Solviet Physics-JETP 27, No. 4, 547 (1968).

Bearden, Alan J., P.L. Mattern, P.S. Nobel. "Mössbauer Effect Apparatus for an Advanced Undergraduate Teaching Laboratory," Am. J. Phys. 32, No. 2, 109 (1964).

Cohen, R.L. "Improvements on Electromagnetic Velocity Drive for Mössbauer Experiments," Rev. Sci. Inst., 37, No. 7, 957 (1966).

Cohen, R.L., P.G. McMullin, G.K. Wertheim. "High Velocity Drive for Mössbauer Experiments," Rev. Sci. Inst. 34, No. 7, 671 (1963).

Flinn, P.A. "Velocity Servo Drive for a High Precision Mössbauer Spectrometer," Rev. Sci. Inst. 34, No. 12, 1422 (1963).

Haskins, J.R. "Advanced Mössbauer-Effect Experiments," Am. J. Phys. 33, No. 8, 646 (1965).

Kankeleit, E., "Simple Mössbauer Spectrometer Using X-Ray Film," Am. J. Phys. 34, No. 9, 778 (1966).

_____. "Velocity Spectrometer for Mössbauer Experiments," Rev. Sci. Inst. 35, No. 2, 194 (1964).

Kock, W.E. "The Mössbauer Radiation," Science 131, 1588 (1960).

Lipkin, J.B., and others. "Inexpensive Automatic Recording Mössbauer Spectrometer," Rev. Sci. Inst. 35, No. 10, 1336 (1964).

Mössbauer, Rudolph L. "Kernresonanzfluoreszenz von Gammastrahlund in Ir^{191}," Die Naturwissenschaften, 45, 538 (1958).

_____. "Kernresonanzfluoreszenz von Gammastrahlung in Ir^{191}," Zeitschrift fur Physik 151, 124 (1958).

_____. "Kernresonanzaborption von Gammastrahlund in Ir^{191}," Z. Naturforsch 14a, 211 (1959).

_____. "Les Prix Nobel En 1961, Nobel Foundation Stockholm, 1962," Science 137, 731 (1962).

_____. "Recoilless Nuclear Resonance Absorption," Annual Review of Nuclear Science 12, 123 (1962).

Pound, R.V., G.A. Rebka, Jr., "Apparent Weight of Photons," Phys. Rev. Letters 4, 337 (1960).

_____. "Variation with Temperature of the Energy of Recoil-Free Gamma Rays from Solids," Phys. Rev. Letters 4, 274 (1960).

Pound, R.V., J.L. Snider. "Effect of Gravity on Gamma Radiation," Phys. Rev. 140, B-788 (1960).

Rubin, David. "Constant Acceleration Transducer Employing Negative Feedback for Use in 'Mössbauer Experiments'," Rev. Sci. Inst. 33, No. 12, 1358 (1962).

Ruegg, F.C., J.J. Spikkerman, J.R. DeVoe. "Drift-Free Mössbauer Spectrometer," Rev. Sci. Inst. 36, No. 3, 356 (1965).

Wertheim, Gunther K. "Mössbauer Effect in Chemistry and Solid-State Physics," Science 144, No. 3616, 253 (1964).

_____. "Resource Letter ME-1 on the Mössbauer Effect," Am. J. Phys. 31, No. 1, 1 (1963).

_____. "The Mössbauer Effect: a Tool for Science," Nucleonics 19, No. 1, 52 (1961).

C. REPORTS

Applications of the Mössbauer Effect in Chemistry and Solid State Physics. Report of a Panel on Applications of the Mössbauer Effect in Chemistry and Solid State Physics. Vienna, April, 1965. Vienna: International Atomic Energy Agency.

Mössbauer Spectra of Organometallic Compounds. Reported by Charles P. Casey (March 3, 1964). Massachusetts Institute of Technology Seminar in Organic Chemistry.

Proceedings of the Dubna Conference on the Mössbauer Effect. New York: Consultants Bureau Enterprises, Inc., (1963).

Proceedings of the Third International Conference on the Mössbauer Effect. Cornell, 1963. Rev. Mod. Phys. 36, 333 (1964).

APPENDIX

APPENDIX

In the determination of the form of the voltage needed by the loud speaker driver, it becomes necessary to know the time dependance of $\dddot{x}$, $\ddot{x}$, $\dot{x}$, and x. For a recycling constant acceleration drive system, the acceleration would be a square wave, except for switching time. This wave form is better approximated by the trapizodial form

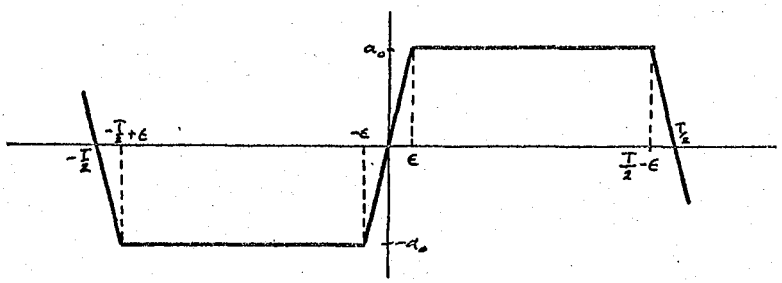

Whose Fourier analysis components are given by:

$$\ddot{X} = \sum_{n=1}^{\infty} b_n \sin\frac{2n\pi t}{T}, \qquad b_n = \frac{4}{T}\int_0^{\frac{T}{2}} f(t) \sin\frac{2n\pi t}{T}\, dt$$

Solving for b_n:

$$b_n = \frac{4}{T}\int_0^{\epsilon}\frac{a_o}{\epsilon}t \sin\frac{2n\pi t}{T}\,dt + \frac{4}{T}\int_{\epsilon}^{\frac{T}{2}-\epsilon} a_o \sin\frac{2n\pi t}{T}\,dt$$
$$+\frac{4}{T}\int_{\frac{T}{2}-\epsilon}^{\frac{T}{2}}\frac{a_o}{\epsilon}\left(\frac{T}{2}-t\right)\sin\frac{2n\pi t}{T}\,dt$$

$$= \frac{a_o T}{\epsilon n^2\pi^2}\left(\sin\frac{2n\pi\epsilon}{T} - \frac{2n\pi\epsilon}{T}\cos\frac{2n\pi\epsilon}{T}\right)$$
$$- \frac{2a_o}{n\pi}\left(\cos\frac{2n\pi}{T}\left(\frac{T}{2}-\epsilon\right) - \cos\frac{2n\pi\epsilon}{T}\right)$$
$$- \frac{a_o T}{\epsilon n\pi}\left(\cos\frac{2n\pi}{T}\frac{T}{2} - \cos\frac{2n\pi}{T}\left(\frac{T}{2}-\epsilon\right)\right)$$
$$- \frac{a_o T}{\epsilon n^2\pi^2}\left(\sin\frac{2n\pi}{T}\frac{T}{2} - \frac{2n\pi}{T}\frac{T}{2}\cos\frac{2n\pi}{T}\frac{T}{2}\right.$$
$$\left. - \sin\frac{2n\pi}{T}\left(\frac{T}{2}-\epsilon\right) + \frac{2n\pi}{T}\left(\frac{T}{2}-\epsilon\right)\cos\frac{2n\pi}{T}\left(\frac{T}{2}-\epsilon\right)\right).$$

Combining like terms and simplifying

$$b_n = \frac{a_0 T}{\epsilon n^2 \pi^2}\left(1 - \cos n\pi\right) \sin \frac{2n\pi\epsilon}{T}$$

$$= \begin{cases} \dfrac{2 a_0 T}{\epsilon n^2 \pi^2} \sin \dfrac{2n\pi\epsilon}{T} , & n = 1, 3, 5, \cdots \\ 0 , & n = 0, 2, 4, \cdots \end{cases}$$

therefore

$$\ddot{x} = \sum_{n\ odd} b_n \sin \frac{2n\pi t}{T}$$

$$= \sum_{n\ odd} \frac{2 a_0 T}{\epsilon n^2 \pi^2} \sin \frac{2n\pi\epsilon}{T} \sin \frac{2n\pi t}{T} ,$$

integrating gives

$$\dot{x} = \int \ddot{x}\, dt$$

$$= -\sum_{n\ odd} \frac{a_0 T^2}{\epsilon n^3 \pi^3} \sin \frac{2n\pi\epsilon}{T} \cos \frac{2n\pi t}{T} ,$$

integrating again

$$x = \int \dot{x}\, dt$$

$$= -\sum_{n\ odd} \frac{a_0 T^3}{2\epsilon n^4 \pi^4} \sin \frac{2n\pi\epsilon}{T} \sin \frac{2n\pi t}{T} ,$$

differentiating $\ddot{x}$ gives

$$\dddot{x} = \frac{d}{dt}\ddot{x}$$

$$= \sum_{n\ odd} \frac{4 a_0}{\epsilon n \pi} \sin \frac{2n\pi\epsilon}{T} \cos \frac{2n\pi t}{T} .$$